

Automated Planning, Exploration and Mapping of Complex Operational Domains of Flight using Multifactor Situational Trees

Ivan Y. BURDUN
INTELONICS Ltd.

Copyright © 2011 SAE International

ABSTRACT

A critical situation can suddenly develop in the ‘pilot (automaton) – aircraft – operational environment’ system behavior as a result of unfavorable mixing and cross-coupling of several demanding operational factors. The latter can include adverse weather effects, pilot (automaton) errors, mechanical failures and hidden design flaws. These factors are typically linked by strong cause-and-effect relationships, which can disturb the normal flow of external forces and moments acting on the aircraft. As a result, a multifactor situation can quickly propagate towards a chain reaction type accident. Specialists (designers, flight test pilots/engineers, regulators, investigators, educators/instructors, line pilots) have limited resources to address multifactor cases during the aircraft life cycle. The main difficulty is combinatorics (‘the curse of dimensionality’) which determines technical, time and budget constraints. Potentially unsafe complex domains of flight can be identified and screened in advance using the system dynamics model as a virtual flight test article. The developed methodology makes it possible to automatically plan, explore, analyze and map a broad set of realistic multifactor scenarios in autonomous fast-time modeling and simulation experiments. The outcome is a situational tree. This is a collection of branching (what-if) flight paths that are specially planted around a baseline situation to thread a complex operational domain of interest. Special techniques are used to mine and granulate the system level flight safety knowledge from these data structures. Multifactor situational trees can be helpful to locate potential anomalies in the system behavior, quantify critical combinations of events and processes (accident precursors), suggest available recovery options, and depict the aircraft’s safety performance under multifactor conditions using ‘a bird’s eye view’ knowledge maps. In this paper, the key concepts, algorithms, data structures, research steps and application examples of the developed methodology are presented using realistic flight cases.

INTRODUCTION

In this section, the research task is formulated: the problem, the solution approach, input requirements and anticipated outcome.

THE PROBLEM

The system under study

Flight safety is an integral characteristic of the ‘operator (human pilot, automaton) – aircraft – operational environment’ system. This is a multi-dimensional non-linear dynamic system with essentially unsteady, stochastic properties. Under certain, very rarely observed circumstances of flight it can exhibit chaotic or even catastrophic behavior if the operational complexity of flight exceeds certain limits. The operational complexity of a flight situation is determined by the number, logic, physical nature and strength of the operational factors, which act concurrently in flight.

The taxonomy of operational factors

In general, the following main groups of the operational factors (conditions, circumstances, effects, etc.), which can occur in flight, can be defined:

$$\Omega(\Phi) = \{\Omega^1(\Phi), \dots, \Omega^{14}(\Phi), \dots\}, \quad (1)$$

where: $\Omega^1(\Phi)$ – a human pilot’s inattention/ carelessness, decision errors, physical incapability or functional inadequacy; $\Omega^2(\Phi)$ – mechanical failures or other malfunctions of the onboard systems or hardware components, which can affect aircraft flight dynamics: the power plant, flight control, undercarriage, etc.; $\Omega^3(\Phi)$ – logic or data errors in automatic flight control algorithms or software; $\Omega^4(\Phi)$ – strong wind effects – including cross wind, tail wind, vertical gusts, horizontal or vertical wind shear, micro bursts, wind rotors, lee waves, etc.; $\Omega^5(\Phi)$ – atmospheric and aircraft wake

turbulence; $\Omega^6(\Phi)$ – heavy rain – impacts on the aircraft aerodynamics, flight dynamics and visibility conditions; $\Omega^7(\Phi)$ – in-flight icing of the aerodynamic surfaces; $\Omega^8(\Phi)$ – non-standard surface conditions of a runway, launch or landing pad – wet, ice- (snow-, or water)-covered, uneven, sloppy, moving; $\Omega^9(\Phi)$ – unfavorable atmospheric state – high temperature or low density; $\Omega^{10}(\Phi)$ – extreme variations of the aircraft weight, moments of inertia and center of gravity location; $\Omega^{11}(\Phi)$ – non-standard changes in the aircraft aerodynamic configuration – e.g. asymmetric flaps extension, etc.; $\Omega^{12}(\Phi)$ – dangerous obstacles located along the projected flight path – terrain, other aircraft; $\Omega^{13}(\Phi)$ – low visibility conditions (nighttime, fog, smoke, etc.); $\Omega^{14}(\Phi)$ – deviations from normal flight path patterns or control tactics. The list $\Omega(\Phi)$ can be further extended and refined – depending on the aircraft class and applications. Meaningful (physics- and logic-wise) combinations of elements Φ_j from the main factor groups (1), which can theoretically occur in flight, represent the anticipated operational environment for aircraft.

Multifactor situations: lack of a priori knowledge

Normally, the effect of a single operational factor from the list $\Omega(\Phi)$ on aircraft dynamics is not critically dangerous, though there are exceptions. Flight safety of a modern aircraft is more likely to be jeopardized by a combined, snow-ball type effect of several demanding operational conditions. ‘Troubles never come alone’. In the course of flight, several operational conditions can mix, adversely and spontaneously, for a very short, 10 to 100 seconds long, period of time. They are often interrelated, both physically and logically.

A multifactor flight situation typically includes a strong cause-and-effect chain of such operational conditions. For instance, in a takeoff situation this can be ‘heavy rain’ ($\Phi_{16} \in \Omega^6(\Phi)$) and/or ‘water covered runway’ ($\Phi_3 \in \Omega^8(\Phi)$), and/or ‘critical engine failure during ground roll’ ($\Phi_{10} \in \Omega^2(\Phi)$), and/or ‘a human pilot error in lateral control’ ($\Phi_2 \in \Omega^1(\Phi)$) and/or ‘an automatic flight controller logic flaw’ ($\Phi_{17} \in \Omega^3(\Phi)$), and so forth. This particular combination $\{\Phi_2, \Phi_3, \Phi_{10}, \Phi_{16}, \Phi_{17}\}$ represents a hypothetical yet realistic five-factor scenario, titled as follows: ‘Continued takeoff with a critical engine out during ground roll in heavy rain and water-covered runway conditions, given pilot errors and possible automatic control logic flaws’. Such operational composites can unpredictably affect the external forces acting on the aircraft, the normal flow of events and processes constituting the aircraft control scenario and thus the overall system dynamics and flight safety. In spite of a negligibly small theoretical probability of occurrence, multifactor cases do happen in flight operations, often leading aircraft to an accident or incident.

It can be stated that the root cause of certain accidents and incidents with modern aircraft is a lack of the system level knowledge about complex operational domains of flight during the design, test, certification, training and operational

phases of the vehicle life cycle. Predictive knowledge about the cause-and-effect mechanisms that govern complex operational domains of flight can go beyond existing requirements. The main difficulty here is combinatorics (‘the curse of dimensionality’), which determines technical, time and budget constraints. The gaps that exist in the ‘internal knowledge base’ of a flight specialist (designer, flight test pilot/test engineer, regulator, educator, investigator, line pilot) with respect to the logic and physics of complex flight domains increase the risk of multifactor accidents in flight operations. Physical and logical patterns of multifactor situations can be very unusual (even anomalous) and thus poorly known a priori. Therefore, a much broader set of multifactor operational scenarios must be examined in advance starting from the earlier design phases.

THE SOLUTION APPROACH

The growing role of modeling, simulation and artificial intelligence

‘Knowledge is Power’. In order to be avoided (or recovered from), a potentially unsafe multifactor scenario of flight must be known in advance and timely recognized onboard. The volume and the quality of a priori knowledge about complex operational domains of flight (gained by specialists, embedded into flight automation or described in piloting manuals) may not be sufficient. Advanced mathematical modeling, computer simulation (M&S) and artificial intelligence (AI) techniques [1] should be employed to a broader extent, starting from the early phases in the aircraft life cycle. The overall goal is to help fill in the gaps of a specialist’s (an automaton’s) ‘internal knowledge base’ about multifactor flight domains. In the presented study, these techniques constitute the basis for an ‘operator (pilot, automaton) – aircraft – operational environment’ system dynamics model.

The system model is employed as a ‘knowledge generator’, or a virtual flight test article, to help explore – in advance and more thoroughly – complex operational domains of flight for a given aircraft or a project. The purpose of the model is to generate virtual flight test and accident statistics under multifactor conditions that cannot be gained in manned simulations, flight tests and operations. By means of the system model (the VATES tool [2]), various multifactor cases including potential anomalies, accident precursors and recovery options can be studied and analyzed in advance.

Main distinguishing feature

‘After all, complicated tasks usually do inherently require complex algorithms, and this implies a myriad of details. And the details are the jungle in which the devil hides. The only salvation lies in structure’ [3]. This guideline by N. Wirth has been implemented in the developed solution approach. The distinguishing feature of the presented methodology is the

structuralization and integration of all the key components of the virtual flight research cycle: concepts, mathematical models, computational algorithms, data structures, software modules, simulation output analysis techniques, and high-level knowledge maps. As a result, it enables the user to automate main labor-consuming steps of the virtual flight research process. These include preparation of the system model's input database, planning of baseline flight scenarios, design of the situational tree structure, modeling and simulation of the aircraft control and flight dynamics, management and analysis of the simulation output database, and granulation and mapping of the system level safety knowledge.

Background and current status

The methodology of virtual flight research in complex conditions is based on the best expertise available in the field of mathematical modeling and computer simulation of flight – see some key publications in [4-9]. Several hundred types of flight situation scenarios have been studied for over 30 aircraft types and projects, including 21 subsonic and four supersonic airplanes, two hypersonic vehicles, three helicopters, one tilt-rotorcraft and one wing-in-ground experimental vehicle.

Using the system model, all major phases and modes of flight can be simulated for various multifactor operational conditions from $\Omega(\Phi)$ in fast-time M&S experiments without a research human pilot in the loop. The classes of simulated situations include flight tests, incidents, accidents, normal operational scenarios, as well as aerobatic, super maneuverable and hypothetical cases. At present, the model functionality is being advanced further to address emerging problems in the field of flight dynamics, control and safety for unmanned aerial and underwater vehicles, wing-in-ground vehicles, hybrid (aerodynamic plus aerostatic) aircraft, and robotic swarms.

INPUT AND OUTPUT

Input requirements

The system model requires the following main input data sets: (1) a 'parametric definition' of the flight vehicle or a project of interest (the aircraft's input characteristics – aerodynamics, moments of inertia, engine thrust, automatic control laws, landing gear kinematics), (2) a list of baseline flight situation scenarios, which will be used as trunks for situational trees, or a general description of the baseline scenarios, (3) a list of the operational factors to be tested, or a general description of the anticipated operational domain, (4) general rules or statistics on the anticipated combinations of operational factors, (5) specifications of the operational constraints to be applied to the analysis and mapping of the system safety performance, and (6) the user general strategy for flight research.

Anticipated output

The following list constitutes the anticipated outcome of the virtual flight research methodology: (1) a set of flight test scenarios, constraints, operational factors and multifactor operational hypotheses, which formally describe the complex operational domain of interest, (2) a database of simulated 'flights' – a 'forest' of situational trees, (3) a family of knowledge maps, which depict the aircraft safety performance for each situational tree, (4) a family of knowledge maps, which depict the individual safety performance of all the branches ('flights') of each situational tree, (5) generalized knowledge on the system level safety performance, including the knowledge of identified potential anomalies, accident precursors (unsafe multifactor operational composites), and safe recovery scenarios (if any), and (6) recommendations on possible control enhancement measures for securing the aircraft flight safety in the given complex operational domain.

Main prerequisite

The main prerequisite for successful application of the system model is the availability of flight physics characteristics for a given aircraft type or project. This input database (the aircraft 'parametric definition') must cover the operational domain of interest including the flight regimes at and beyond constraints. However, the accuracy and 'richness' level of the aircraft 'parametric definition' does not exceed the requirements that are applicable to the input database of a manned flight simulator used for engineering or training tasks.

COMPLEX FLIGHT DOMAIN MODEL

In this section, a framework of key concepts, data structures and algorithms, which constitute the developed methodology of virtual flight testing under complex operational conditions, is introduced. Then, M&S experiment setup and simulation output are described for major phases and realistic multifactor operational conditions of flight.

CONCEPTUAL FRAMEWORK

Key concepts

A generalized conceptual M&S framework has been developed for aircraft safety performance mapping, analysis, prediction and protection under multifactor conditions. These concepts are independent of the aircraft type, flight situation and operational conditions. The developed theoretical framework includes the following key concepts [11, 12]: system model, event, process, scenario, micro- and macro-structure of flight, baseline scenario, operational (design) factor, operational hypothesis, situational tree, safety palette, partial safety spectra, integral safety spectrum, safety

classification categories, safety window, family of the integral safety spectra of a situational tree, and some other.

Representation of flight M&S data

The ‘operator (pilot, automaton) – aircraft – operational environment’ system (the system) behavior is described as an ordered set of the system states $\mathbf{x}(t)$, $\mathbf{x}(t) = \{x_1(t), \dots, x_i(t), \dots, x_{N(x)}(t)\}$, where x_i is a system variable, $x_i \in \mathbf{x}$, $t \in [t^*; t^*]$. This data sequence is called a ‘flight’ (F_k),

$$F_k = \{ \{x_1(t^*), \dots, x_{N(x)}(t^*)\}, \dots, \{x_1(t^* + (n-1)\Delta), \dots, x_{N(x)}(t^* + (n-1)\Delta)\} \}, \quad (2)$$

where n is the total number of data records in F_k , $t^* = t^* + (n-1)\Delta$, and Δ is the time increment of updating the output data file (the ‘flight’ F) in M&S experiments.

Micro-structure and macro-structure of flight

Safety knowledge of a complex flight situation domain is studied on two interconnected levels. These are the ‘micro-structure’ of flight (a flight situation scenario) and the ‘macro-structure’ of flight (a situational tree). The relationship between these knowledge structures is shown in Figure 1.

The micro-structure of flight is a generalized model of a stand-alone (single) flight situation. It can be represented by the concept of flight situation scenario \mathbf{S} . The latter is basically a directed graph, which consists of interconnected events and processes. In the scenario graph, a flight event (a vertex) \mathbf{E} stands for a discrete component of the flight situation model, whilst a flight process (a directed arc) $\mathbf{\Pi}$ stands for its continuous component. In other words, the formal scenario is a preplanned data structure designed to capture key cause-and-effect, time, instrumental and other logic relationships of flight dynamics and control in a given flight situation [1].

The macro-structure of flight is a knowledge model of a family of neighboring (what-if) situations. It can be represented, planted, stored and used in safety research as a tree. The tree trunk stands for some baseline flight situation – standard or non-standard one. Secondary (n^{th} -order derivative) branches represent multifactor situations, which implement meaningful variations of the baseline scenario or derivative scenarios of a lower level. New branches are automatically ‘implanted’ into the tree using the VATES v.7 M&S tool [2].

Operational factor and operational hypothesis

The operational factor Φ is some event or process (or its attribute), which can be added to or withdrawn from a baseline (or derivative) flight situation scenario, $\Phi \in \Omega(\Phi)$. Operational factors may vary substantially and independently in flight and thus can improve or deteriorate flight safety. Typically, an

operational factor Φ is defined by a single system variable x_i , $x_i \in \mathbf{x}$. Operational factors are used in M&S experiments to generate multifactor derivative branches in a situational tree. Each derivative ‘flight’ from the tree corresponds to one combination of operational factors Φ_j .

It is important to study the effects of various combinations of operational factors on flight safety in advance. A meaningful combination (a composite) of several operational factors is called the operational hypothesis. In the model, the operational hypothesis Γ is used as a formal rule to incorporate a new operational composite into a baseline scenario. Formally, the operational hypothesis can be defined as follows:

$$\Gamma = \prod_{i=1}^n \left[\sum_{k=1}^m \Phi_k^i \right], \quad (3)$$

where Φ_k^i is the k^{th} dependent factor added to the baseline scenario on the i^{th} independent level of the situational tree branching process, $i = 1, \dots, n$, $k = 1, \dots, m$. In (3), Π is the symbol of Cartesian product (independent combination), and Σ is the symbol of dependent (cross-coupled) combination of operational factor values Φ_k^i on the i^{th} level.

Situational tree as knowledge base

A situational tree \mathfrak{S} is a composition of a baseline situation scenario \mathbf{S} and a multifactor operational hypothesis Γ :

$$\mathfrak{S} = \mathbf{S} \cdot \Gamma \equiv \Omega(F). \quad (4)$$

The tree \mathfrak{S} is generated in M&S experiments with the system model. It can be viewed as a ‘what-if neighborhood’ of the baseline situation, i.e. as a structured set of branching situations F_k that surround \mathbf{S} . In other words, the rule (4) is the situational tree ‘genotype’ that determines its shape, size, branching properties and safety characteristics. Each situation-branch \mathbf{B} (a ‘flight’ F_k), $\mathbf{B} \in \mathfrak{S}$, is defined by a combination of contributing operational factors Φ_j (the rule Γ), the baseline scenario \mathbf{S} , and the system dynamics.

The goal of constructing a situational tree is to examine the combined effect of demanding operational conditions on the aircraft’s safety performance and thus to generate in advance missing statistics on possible multifactor accident patterns. The overall goal of virtual flight test research process is to construct a ‘forest’ of such trees and to analyze safety properties of the complex flight situation domain it threads based on available design, test, operation or incident data.

Safety palette. Fuzzy flight constraints

Color is a natural and efficient medium for storing and communicating safety-related information. Five basic colors

(green ξ_G , yellow ξ_Y , red ξ_R , black ξ_B and grey/white ξ_W) are used to denote respectively ‘normal’, ‘warning’, ‘dangerous’, ‘catastrophic’ and ‘uncertain’ levels of the system safety performance for each measured system variable x_i from (2) and each time instant t recorded in flight – see Figure 2 (a).

Operational constraints of flight under multifactor conditions are not known precisely. They are inherently fuzzy. In the system model, the notion of fuzzy constraint introduced by L.A. Zadeh is employed for approximate measurement of the compatibility of current system states, measured at time instants t , with operational constraints using key system variables (monitored flight parameters). A notional example of the fuzzy constraint for the angle of attack α is presented in Figure 2 (b), together with a scheme for coloring its numeric definition domain using the safety palette from Figure 2 (a).

Safety spectra

For each flight situation from a situational tree, its current safety levels can be measured at all recorded time instants for all monitored variables x_k . As a result, for each situation, a family of partial safety spectra $\Sigma_k, k = 1, \dots, N$, and an integral safety spectrum Σ can be constructed using the following general algorithm:

$$\begin{aligned} & (\forall t) (t \in [t^*; t^*]) (\exists \xi(x_k(t)) (x_k \in X \wedge x_k(t) \in F) \\ & (\xi(x_k(t)) \in \{\xi_G, \xi_Y, \xi_R, \xi_B, \xi_W, \dots\} \wedge (\xi_B < \xi_R < \xi_Y < \xi_G < \xi_W)) \\ & (\xi(t) = \max \xi(x_k(t)), k = 1, \dots, N) \Rightarrow (\xi(t) \in \Sigma \wedge \\ & \Sigma = \xi(t^*) \parallel \xi(t^* + \Delta) \parallel \xi(t^* + 2 \cdot \Delta) \parallel \dots \parallel \xi(t^*) \end{aligned} \quad (5)$$

where \max denotes the operation of selecting the ‘hottest’ color from the safety colors recorded for all monitored variables x_k at a time instant t , $<$ is the operation of comparing safety colors, and \parallel is the operation of geometric concatenation for two sequential safety color bars [11, 12].

The integral safety spectrum is basically a color-coded time-history of the situation safety status, which maps all cases of the violation and restoration of monitored fuzzy constraints during a flight situation at the ‘hottest’ level taking into account the available partial safety spectra. A more detailed introduction to the technique of flight safety spectra construction and applications can be found in [11, 12]. Examples of partial safety spectra and an integral safety spectrum are shown in Figure 3 for a ‘flight’ F_{2237} : ‘Continued takeoff and initial climb of an airplane at a commanded flight path angle (θ_G) of 5° and commanded bank angle (γ_G) of -42° with the left-hand engine out during ground-roll’.

Safety Classification Categories

One more level of flight safety knowledge generalization is needed in addition to the notion of safety spectra. The goal is to measure the aircraft’s safety performance in a particular flight situation as a whole. With this purpose, a generalized

‘safety ruler’ that consists of six safety classification categories is introduced (Table 1).

Table 1 – Flight situation safety classification categories

Code	Name	Definition
I	Safe	The system state resides mainly inside the ‘green’ zone. As a maximum, the system state may stay, for a short time in close proximity to the operational constraints, i.e. inside the ‘yellow’ zone, but must leave it by the end of the situation
II-a	Conditionally Safe – a	As a maximum, the system state may stay temporarily, or for a medium time, in close proximity to the operational constraints, i.e. inside the ‘yellow’ zone
II-b	Conditionally Safe – b	As a maximum, the system state may stay for a long time in close proximity to the operational constraints, i.e. inside the ‘yellow’ zone
III	Potentially Unsafe	As a maximum, the system state may violate operational constraints, i.e. enter the ‘red’ zone, for a short or between short and medium time, but must leave it by the end of the situation
IV	Dangerous (Prohibited)	As a maximum, the system state may stay beyond the operational constraints, i.e. inside the ‘red’ zone, for a medium or long time or till the end of the situation
V	Catastrophic (‘Chain Reaction’)	There is at least one (i.e. for a very short time) occurrence of the violation of any operational constraint at the ‘black’ level

This classification algorithm (Table 1) takes into account the palette, the ‘weight’ and the position of the four basic safety colors $\{\xi_G, \xi_Y, \xi_R, \xi_B\}$ in the integral safety spectrum Σ of a flight situation $F_k, F_k \in \Omega(F)$. Two new colors (‘salad green’ and ‘orange’) have been added to the original safety palette to denote interim categories: **II-a** and **III**, respectively. In general, the proposed total number of the flight safety classification categories in Table 1 (six) corresponds to a human expert’s ability to reliably recognize and utilize five to ten levels of a complex, difficult-to-formalize system property. This technique is based on the concept of ‘information granulation’ introduced by L.A. Zadeh [10].

The main criterion for assigning a safety category ξ_k from Table 1, $\xi_k \in \{\xi_I, \xi_{II-a}, \xi_{II-b}, \xi_{III}, \xi_{IV}, \xi_V\}$, to a flight situation F_k is the relative residence time of the system state, respectively, in the ‘green’, ‘salad green’, ..., and ‘black’ zones of this situation’s integral safety spectrum. As a result, for each situation-branch from a tree $\mathfrak{F}, \mathfrak{F} \equiv \Omega(F)$, a qualitative safety level (safety category) can be assigned. Such generalized safety color codes or grades are expedient to have for predictive and post-event flight safety analysis and in-flight decision-making support in complex operational domains.

Safety Window

Let us have a situational tree of ‘flights’ $\Omega(F), \Omega(F) = \{F_{(1),(1)}, \dots, F_{(i),(j)}, \dots, F_{(m),(n)}\}$ with the following pairs of values for two key operational factors Φ_a and Φ_b :

$$\{(\Phi_{a(1)}, \Phi_{b(1)}), \dots, (\Phi_{a(i)}, \Phi_{b(j)}), \dots, (\Phi_{a(m)}, \Phi_{b(n)})\}, \quad (6)$$

where $\Phi_{a(1)} > \Phi_{a(2)} > \dots > \Phi_{a(m)}$ is a top-to-bottom vertical ordering relation for the values of the first factor Φ_a and $\Phi_{b(1)} < \Phi_{b(2)} < \dots < \Phi_{b(n)}$ is a left-to-right horizontal ordering relation for the values of the second key factor Φ_b . Then, a flight safety window can be defined as a $m \times n$ matrix $W(\Phi_a, \Phi_b)$ with the coordinates Φ_a and Φ_b , where w_{ij} is a cell located on the crossing of the row $\#i$ and column $\#j$,

$$w_{ij} = [(\Phi_{a(i)}, \Phi_{b(j)}), \xi_{ij}^k], \quad (7)$$

$i = 1, \dots, m, j = 1, \dots, n, k \in \{\mathbf{I}, \dots, \mathbf{V}\}$. The cell w_{ij} contains the following information: $\Phi_{a(i)}, \Phi_{b(j)}$ – a pair of values of factors (Φ_a, Φ_b) , where $\Phi_{a(i)} = \text{const}$ for $(\forall i) (i = 1, \dots, m)$ and $\Phi_{b(j)} = \text{const}$ for $(\forall j) (j = 1, \dots, n)$, and ξ_{ij}^k – the color of the k^{th} cluster, which the ‘flight’ $F_{(i,j)}$ belongs to, $k \in \{\mathbf{I}, \dots, \mathbf{V}\}$, $\xi_{ij}^k \in \{\xi^{\mathbf{I}}, \dots, \xi^{\mathbf{V}}\}$. The VATES tool incorporates an algorithm for automatic mapping of all the ‘flights’ from a tree $\Omega(F)$, $\Omega(F) = \mathbf{S} \cdot \Gamma$, on to a safety window plane $W(\Phi_a, \Phi_b)$.

SIMULATION EXPERIMENT SETUP

Virtual flight research process

The developed virtual flight test process is carried out as a sequence of the following main research steps:

1. Develop the aircraft ‘parametric definition’ and implement the system dynamics model using VATES.
2. Plan and debug the baseline flight situation scenarios.
3. Formalize a subset of the operational factors selected for testing in M&S experiments.
4. Plan a situational tree’s ‘genotype’ – a multifactor operational hypothesis.
5. Select a subset of the output color-coded graphic maps to be used for flight safety knowledge mapping.
6. Debug and validate the system model using available real or simulated flight data for the given vehicle or prototype.
7. Run a series of autonomous flight M&S experiments to test the multifactor operational hypothesis and construct a situational tree.
8. Map time-histories of the what-if ‘flights’ from the tree by means of the selected knowledge maps.
9. Screen the multifactor situational space of flight using the selected knowledge maps.
10. Mine new knowledge ‘granules’ of the system safety performance in multifactor situations from M&S experiment data and knowledge maps.
11. Identify and quantify possible anomalies, unsafe control scenarios and accident precursors in the system dynamics.
12. Identify and quantify safe situations, their precursors and control scenarios.

13. Explore in depth accident avoidance or recovery control techniques (or remedial design solutions) to avoid chain reaction type accidents (anomalies) under multifactor operational conditions.
14. Issue recommendations on the aircraft flight safety performance and refine operational constraints, human piloting tactics and automatic control laws for the given (multifactor) operational domain.

Aircraft 6-DOF flight dynamics model

Using the methodology and research process described above, a series of M&S experiments has been planned and carried out with the system model to study takeoff, climb, level, descent, landing approach, go-around and landing phases of flight in multifactor conditions for a notional commuter airplane. The quality and the ‘richness’ of the vehicle ‘parametric definition’ used to build its 6-DOF non-linear flight dynamics model matches the input data requirements applicable to engineering and training flight simulators.

Baseline flight situation scenarios

Seven baseline flight situation scenarios $\{\mathbf{S}_1, \dots, \mathbf{S}_7\}$ have been developed for demonstration. These are as follows (Table 2): \mathbf{S}_1 : ‘Normal takeoff and initial climb’, \mathbf{S}_2 : ‘Continued takeoff and initial climb with left-hand engine out during ground-roll’, \mathbf{S}_3 : ‘Continued takeoff and initial climb in cross wind conditions with left-hand engine out during ground-roll on wet runway’, \mathbf{S}_4 : ‘Level flight followed by climb or descent’, \mathbf{S}_5 : ‘Landing approach and go-around in wind shear conditions’, \mathbf{S}_6 : ‘Landing approach and go-around in wind shear conditions with left-hand engine out’, and \mathbf{S}_7 : ‘Landing approach, landing and ground-roll’. Note that the scenario subset $\{\mathbf{S}_2, \mathbf{S}_3, \mathbf{S}_5, \mathbf{S}_6\}$ already represents non-standard cases with non-empty subsets of operational factors.

Table 2 – Baseline flight situation scenarios, $\Omega(\mathbf{S})$

Symbol and name	$\Omega_a(\Phi)$	$N(\Omega_a(\Phi))$
\mathbf{S}_1 : Normal takeoff and initial climb	\emptyset	0
\mathbf{S}_2 : Continued takeoff and initial climb with left-hand engine out during ground-roll	$\{\Phi_{10}\}$	1
\mathbf{S}_3 : Continued takeoff and initial climb in cross wind conditions, with left-hand engine out during ground-roll on wet runway	$\{\Phi_3, \Phi_4, \Phi_{10}\}$	3
\mathbf{S}_4 : Level flight followed by climb or descent	\emptyset	0
\mathbf{S}_5 : Landing approach and go-around in wind shear conditions	$\{\Phi_6\}$	1
\mathbf{S}_6 : Landing approach and go-around in wind shear conditions with left-hand engine out	$\{\Phi_6, \Phi_{11}\}$	2
\mathbf{S}_7 : Landing approach, landing and ground-roll	\emptyset	0
Note. See Table 9 for definitions of Φ_i .		

These baseline situations represent central branches (‘trunks’) of the multifactor situational trees, which will be generated and tested in M&S. The scenarios \mathbf{S}_1 , \mathbf{S}_2 and \mathbf{S}_3 stand for normal and continued takeoff situations under benign and

demanding (cross wind) conditions. The scenario S_4 consists of a level flight phase followed by descent or climb after a decision-making point. The scenarios S_5 and S_6 begin with a landing approach phase, followed by climb after reaching a ‘go-around’ decision point – either in benign weather or wind shear conditions. Finally, the scenario S_7 represents a standard landing situation and is composed of the approach, landing and ground roll phases. Specified below are the lists of the events and processes (control procedures, mechanical failures, piloting tasks, state observers, and demanding weather conditions), which constitute $\Omega(S)$, $\Omega(S) = \{S_1, \dots, S_7\}$.

Flight events

A united calendar $\Omega(E)$ of all the flight events that form a discrete framework for the scenarios $\Omega(S)$ is defined in Table 3. It is essential that the recognition criteria developed for the events from $\Omega(E)$ are sufficiently general to formalize realistic flight situations, manual piloting and automatic control tactics. Note that about 30 events are sufficient to formalize all major phases of flight for a civil airplane – from takeoff to landing.

Table 3 – Flight events, $\Omega(E)$

Symbol and name	E^{IF}	Recognition criterion			
		x	\square	A	U
E_1 : start		t	\geq	t^*	s
E_2 : LEO speed	E_1	IAS	\geq	V_{EF}	km/h
E_3 : VR achieved		IAS	\geq	V_R	km/h
E_4 : pitch 7 degr.	E_3	ϑ	\approx	7	°
E_5 : in airborne	E_3	$R_{LG2} + R_{LG3}$	$=$	0	kN
E_6 : altitude 10.7 m		H	\geq	10.7	m
E_7 : altitude 120 m		H	\geq	120	m
E_8 : flaps retracted		δ_f	$=$	0	°
E_9 : decision point		t	\geq	30	s
E_{10} : high speed	E_9	IAS	\geq	390	km/h
E_{11} : go-around decision		H	\leq	30	m
E_{12} : positive climb rate	E_{11}	\dot{H}	\geq	0.5	m/s
E_{13} : safe altitude	E_8	H	\geq	150	m
E_{21} : altitude to flare		H_w	\leq	9	m
E_{22} : load factor ≥ 1.15	E_{21}	n_z	\geq	1.15	-
E_{23} : small descent rate		\dot{H}	\geq	-1.0	m/s
E_{24} : touchdown	E_{21}	$s_2 \vee s_3$	\geq	0.01	m
E_{25} : touchdown + 5s delay		t	\geq	$t(E_{24}) + 5$	s
E_{26} : IAS 100 km/h	E_{24}	IAS	\approx	100	km/h
E_{27} : IAS 30 km/h	E_{26}	IAS	\approx	30	km/h
E_{99} : stop		t	$>$	t^*	S

Note. More complex (compound) recognition criteria, such as $(x \square A)_1 \nabla (x \square A)_2 \nabla \dots \nabla (x \square A)_n$, are not shown. $\nabla \in \{\wedge, \vee\}$, $x \in x$.

Flight processes

In addition to the calendar of events $\Omega(E)$, the following lists of flight processes have been compiled to fill in the baseline scenarios $\Omega(S)$: $\Omega(P) \cup \Omega(F)$ – a united list of control procedures and mechanical malfunctions, $\Omega(T)$ – a list of piloting tasks, $\Omega(O)$ – a list of system state observers, and $\Omega(Y) \cup \Omega(W)$ – a united list of weather related processes. The

control procedures and mechanical malfunctions, $\Omega(P)$ and $\Omega(F)$, are formalized in Table 4. The piloting tasks $\Omega(T)$ and the associated system state observers $\Omega(O)$ that represent manual flight control with continuous feedback are defined in Tables 5 and 6. Weather related processes, $\Omega(Y) \cup \Omega(W)$, which simulate demanding (wet) runway conditions, cross wind and wind shear conditions, are specified in Tables 7 and 8. It follows from the presented examples that M&S scenarios for major phases of flight can be formalized in a uniform fashion for the purpose of complex flight domains analysis using a simple (‘events-processes’) description language.

Table 4 – Control procedures and mechanical malfunctions, $\Omega(P)$ and $\Omega(F)$

Symbol and name	Control vector, u	Goal, u_G	U	Rate of change
P_1 : throttles → takeoff power	δ_{T1}, δ_{T2}	100	%	s
P_2 : elevator → up	δ_e	-8	°	m
P_3 : wheels → up	δ_w	0	-	n
P_4 : flaps → up	δ_f	0	°	n
P_5 : airbrake → on	$\delta_{A,BR}$	60	°	n
P_6 : elevator → down	δ_e	15	°	s
P_7 : throttles → idle	δ_{T1}, δ_{T2}	7	%	n
P_8 : ground spoilers → on	$\delta_{GR,SP}$	50	°	n
P_9 : wheel brakes → on	$\delta_{W,BR}$	1	-	n
P_{10} : throttles → reverse	δ_{T1}, δ_{T2}	-60	%	n
P_{11} : throttles → idle	δ_{T1}, δ_{T2}	7	%	n
P_{12} : wheel brakes → off	$\delta_{W,BR}$	0	-	n
P_{13} : ground spoilers → off	$\delta_{GR,SP}$	0	°	n
P_{14} : ailerons & rudder → neutral	δ_a, δ_r	0	°	m
F_1 : left-hand engine failure	δ_{T2}	-5	%	f

Note. $u \subset x$; s – slow, m – medium, n – normal, f – fast.

Table 5 – Piloting tasks, $\Omega(T)$

Symbol and name	Control vector, u	State observer	Main observed variables, y
T_1 : steer runway centerline	$\delta_{N,W} / \delta_f$	O_1	ψ
T_2 : maintain initial climb path	δ_e	O_2	θ
T_3 : control sideslip & bank	δ_s, δ_b	O_3	β, γ
T_4 : maintain IAS	δ_{T1}, δ_{T2}	O_4	IAS
T_5 : control heading & bank	δ_r, δ_b	O_5	ψ, γ
T_6 : maintain initial climb path	δ_e	O_6	θ
T_7 : maintain level flight	δ_e	O_7	\dot{H}
T_8 : maintain IAS	δ_{T1}, δ_{T2}	O_8	IAS
T_9 : maintain flight path	δ_e	O_9	θ
T_{10} : maintain glide slope	δ_e	O_{10}	\dot{H}
T_{11} : maintain tangent path	δ_e	O_{11}	\dot{H}

Note. $u \subset x$, $y \in y$, $y \in x$. See Table 6 for definitions of O_i .

Table 6 – System state observers, $\Omega(O)$

Symbol and name	State observation vector(s), y	Goal, y_G	U
O_1 : observe heading & bank	$(\psi, \dot{\psi}, r), (\gamma, \dot{\gamma}, p)$	0	°
O_2 : observe climb path	$(\theta, \dot{\theta}, q)$	8	°
O_3 : observe sideslip & bank	$(\beta, \dot{\beta}, r), (\gamma, \dot{\gamma}, p)$	0	°
O_4 : observe IAS	(IAS, \dot{V})	250	km/h
O_5 : observe heading & bank	$(\psi, \dot{\psi}, r), (\gamma, \dot{\gamma}, p)$	0	°

\mathbf{O}_6 : observe climb path	$(\theta, \dot{\theta}, q)$	5	$^\circ$
\mathbf{O}_7 : observe flight path	(\dot{H}, \ddot{H}, q)	0	m/s
\mathbf{O}_8 : observe IAS	(IAS, \dot{V})	300	km/h
\mathbf{O}_9 : observe flight path	$(\theta, \dot{\theta}, q)$	5	$^\circ$
\mathbf{O}_{10} : observe descent rate	(\dot{H}, \ddot{H}, q)	-3.5	m/s
\mathbf{O}_{11} : observe descent rate	(\dot{H}, \ddot{H}, q)	-0.2	m/s
Note. $y \subset x$.			

Table 7 – Weather related processes, $\Omega(\mathbf{Y})$ and $\Omega(\mathbf{W})$

Symbol and name	Variables	Function
\mathbf{Y}_1 : wet runway conditions	μ_D	$f(F)$ – see Table 13
\mathbf{W}_1 : cross wind conditions	W_{yg}	$f(t)$ – see Table 8
\mathbf{W}_2 : wind shear conditions	W_{xg}, W_{zg}	$f(t)$ – see Table 8
Note. $(\forall t)(t \in [t^*, t^*])(\mathbf{W}_1 \Rightarrow W_{xg}, W_{zg} = 0; \mathbf{W}_2 \Rightarrow W_{yg} = 0)$.		

Table 8 – Specification of wind type processes, $\Omega(\mathbf{W})$

Π	Variable		Piecewise linear function node #										\mathfrak{Z}_i	
	x	U	1	2	3	4	5	6	7	8	9	10		
\mathbf{W}_1	t	s	0	3	10	20	t^*	-	-	-	-	-	-	\mathfrak{Z}_1
	W_{yg}	m/s	0	10	10	10	t^*	-	-	-	-	-	-	\mathfrak{Z}_3
\mathbf{W}_2	t	s	0	10	15	19	27	35	41	46	53	t^*	\mathfrak{Z}_5	
			0	10	12	16	24	32	42	47	55	t^*	\mathfrak{Z}_6	
			0	10	12	16	24	32	38	43	50	t^*	\mathfrak{Z}_7	
			0	10	15	25	37	45	55	60	64	t^*	\mathfrak{Z}_8	
	W_{xg}	m/s	0	-7	-12	-8	-14	-12	2	6	3	2.5	\mathfrak{Z}_k	
W_{zg}	m/s	0	0	0	0	-1	-1	-2.5	-3	-1	0	\mathfrak{Z}_k		
Note. See Table 11 for definitions of $\mathfrak{Z}_i; k \in \{5, \dots, 8\}$.														

Scenario graphs and description

Scenario \mathbf{S}_1 : ‘Normal takeoff and initial climb’ (Figure 4). The situation begins at the event \mathbf{E}_1 , with the aircraft positioned on the runway ready for takeoff. At this point, both throttles (δ_{T1}, δ_{T2}) are moved to a takeoff power setting by means of the control procedure \mathbf{P}_1 . Simultaneously, the ‘silicon pilot’ begins to monitor and control the ground roll path by means of the two interrelated processes – the state observer \mathbf{O}_1 and the piloting task \mathbf{T}_1 . The observer \mathbf{O}_1 is employed to measure the aircraft heading angle (Ψ) error with respect to the runway centerline and the aircraft bank angle (γ) error. In the piloting task \mathbf{T}_1 , the ‘pilot’ maintains the runway centerline using rudder and nose wheel steering. When a rotation speed V_R is reached (at \mathbf{E}_3), elevator is deflected up by -8° using the process \mathbf{P}_2 to rotate the aircraft. Once the nose wheel is off the runway (at \mathbf{E}_4), the processes of ground roll motion observation and control ($\mathbf{O}_1, \mathbf{T}_1$) are terminated. At a pitch attitude (ϑ) of about 7° nose up (\mathbf{E}_4), the pilot commences the processes of monitoring and maintaining the initial climb path; these are the observer \mathbf{O}_2 and the task \mathbf{T}_2 . Here, the commanded initial climb path is attained and maintained by means of elevator (δ_e) using the flight path angle (θ) error measurements. Shortly after lift-off (at \mathbf{E}_5), the process of monitoring the aircraft sideslip (β) and bank (γ) angles begins (\mathbf{O}_3). It is used to provide real-time system state error feedback for the process \mathbf{T}_3 of the aircraft lateral control

by means of rudder (δ_r) and ailerons (δ_a). At an altitude of 10.7 meters (\mathbf{E}_6), the wheels are retracted ($\delta_w: 1 \rightarrow 0$) using the procedure \mathbf{P}_3 . When a safe altitude of 120 m is reached (\mathbf{E}_7), flaps are retracted (\mathbf{P}_4). Once the aircraft is in clean configuration (at \mathbf{E}_8), the following pairs of state observers and piloting tasks are commenced: ($\mathbf{O}_4, \mathbf{T}_4$) – to maintain a commanded value of indicated airspeed (IAS) by means of throttles, ($\mathbf{O}_5, \mathbf{T}_5$) – to steer commanded heading and bank angles by means of rudder and ailerons, and ($\mathbf{O}_6, \mathbf{T}_6$) – to maintain a new commanded flight path angle by means of elevator during the second phase of initial climb after flaps retraction. The situation is ended at the stop event \mathbf{E}_{99} ($t > t^*$).

Scenario \mathbf{S}_2 : ‘Continued takeoff and initial climb with left-hand engine out during ground-roll’ (Figure 4). This scenario is structurally close to \mathbf{S}_1 , with only a new event \mathbf{E}_2 (a left-hand engine out airspeed) added between the events \mathbf{E}_1 and \mathbf{E}_3 to simulate the engine failure process \mathbf{F}_1 during ground roll ($\zeta_2: 1 \rightarrow 0$, or $\delta_{T2}: \delta_{T2}(t) \rightarrow -5\%$).

Scenario \mathbf{S}_3 : ‘Continued takeoff and initial climb with left-hand engine out during ground-roll in wet runway and cross wind conditions’ (Figure 4). This is a more complex scenario that repeats \mathbf{S}_2 with two new processes, \mathbf{Y}_1 and \mathbf{W}_1 , added at the start event \mathbf{E}_1 to represent demanding weather. These processes simulate the effects of a wet runway condition (\mathbf{Y}_1) and a cross wind condition (\mathbf{W}_1) on the aircraft behavior with the left-hand engine failed during ground roll at V_{EF} (\mathbf{E}_2).

Scenario \mathbf{S}_4 : ‘Level flight followed by climb or descent’ (Figure 5). This is a simple scenario with only four events and seven control processes. Its physical content and logical structure (the events-processes relationships) are clear from the directed graph depicted in Figure 5.

Scenario \mathbf{S}_5 : ‘Landing approach and go-around in wind shear conditions’ (Figure 6). This scenario has a simple logical structure with only three interim events $\{\mathbf{E}_{11}, \mathbf{E}_{12}, \mathbf{E}_{13}\}$. The piloting tasks $\{\mathbf{T}_2, \mathbf{T}_3, \mathbf{T}_4, \mathbf{T}_5, \mathbf{T}_8, \mathbf{T}_{10}\}$ and the associated state observers, together with the standard control procedures $\{\mathbf{P}_1, \mathbf{P}_3, \mathbf{P}_4\}$, are coherently employed to attain and maintain the commanded values of the aircraft flight path (θ_G), bank attitude (γ_G) and indicated airspeed during the approach and go-around phases. Note that the wind shear process \mathbf{W}_2 affects the entire situation with the maximum airspeed loss occurred during the first portion of the go-around phase (see Table 8).

Scenario \mathbf{S}_6 : ‘Landing approach and go-around in wind shear conditions with left-hand engine out’ (Figure 6). This scenario repeats \mathbf{S}_5 with one new process added (\mathbf{F}_1). The latter simulates the left-hand engine failure occurred at \mathbf{E}_{12} , when the aircraft has just established a positive rate of climb.

Scenario \mathbf{S}_7 : ‘Landing approach, landing and ground-roll’ (Figure 7). This is a manual control intensive scenario designed to simulate a typical landing sequence. It includes

the phases of landing approach, landing and ground roll. The logic of this scenario is based on nine events, ten control procedures, five piloting tasks and five associated state observers. Its structure and content are clear from the graph.

Operational factors

Table 9 contains a united list of the operational factors, which formalize the complex operational domains of flight selected for testing in M&S. The effect of each operational factor from $\Omega(\Phi)$ is modeled by one system variable – as an attribute of a modified flight event or flight process.

Table 9 – Operational factors, $\Omega(\Phi)$

Symbol and name	Scenario element and attribute	
	ε	x
Φ_1 : commanded flight path angle	O	θ_G
Φ_2 : commanded bank angle	O	γ_G
Φ_3 : wheels-runway adhesion factor	I	μ_D
Φ_4 : cross wind velocity	W	W_{yg}
Φ_5 : go-around thrust rating	P	P_{GA}
Φ_6 : wind shear intensity	W	k_W
Φ_7 : flaps-up delay	P	$\tau(\delta_F)$
Φ_8 : thrust-increase delay	P	$\tau(P_{max})$
Φ_9 : commanded descent rate	O	\dot{H}_G
Φ_{10} : LEO at V_{EF}	F	δ_{T2}
Φ_{11} : LEO in go-around	F	δ_{T2}
Φ_{12} : right-hand engine thrust increase rate	P	\dot{P}
Φ_{13} : flare start altitude	E	H_{FL}
Φ_{14} : elevator-up increment	P	$\Delta\delta_e$
Φ_{15} : commanded descent rate before touchdown	O	\dot{H}_{G1}

Note. $x \in x$. See corresponding tables above for definitions of ε_i .

Operational hypotheses

Seven operational hypotheses $\{\Gamma_1, \dots, \Gamma_7\}$ have been designed to represent several realistic combinations of the operational factors from $\Omega(\Phi)$. Other operational composites can be easily derived within the given M&S setup. The design formula and the number of contributing factors for each hypothesis from $\{\Gamma_1, \dots, \Gamma_7\}$ are defined in Table 10. Note that the operational factors from the scenarios $\{S_2, S_3, S_5, S_6\}$ are not included here. It is essential that an operational hypothesis must represent a meaningful combination of the operational factors and reflect an interrelated physical and logical structure of the operational domain of interest – either a hypothetical one or a ‘neighborhood’ of some accident happened in the past.

Table 10 – Operational hypotheses, $\Omega(\Gamma)$

Symbol and name	Definition formula	$N(\Phi)$
Γ_1 : Errors in selecting (or variations of) commanded flight path and bank angles	$\Phi_1 \times \Phi_2 \equiv \theta_G \times \gamma_G$	2
Γ_2 : Variations of wheels-runway adhesion	$\Phi_3 \times \Phi_4 \times \Phi_1 \equiv$	3

factor, cross wind velocity, and commanded flight path angle	$\mu_D \times W_{yg} \times \theta_G$	
Γ_3 : Errors in selecting (or variations of) go-around thrust rating, and commanded flight path and bank angles	$\Phi_5 \times \Phi_1 \times \Phi_2 \equiv P_{GA} \times \theta_G \times \gamma_G$	3
Γ_4 : Variations of wind shear intensity, and commanded flight path and bank angles	$\Phi_6 \times \Phi_1 \times \Phi_2 \equiv k_W \times \theta_G \times \gamma_G$	3
Γ_5 : Errors in selecting (or variations of) go-around thrust increase delay, commanded flight path angle and flaps-up delay	$\Phi_8 \times \Phi_1 \times \Phi_7 \equiv \tau(P_{max}) \times \theta_G \times \tau(\delta_F)$	3
Γ_6 : Errors in selecting (or variations of) commanded rate of descent, commanded flight path and bank angles, and right-hand engine thrust increase rate in climb	$\Phi_9 \times \Phi_1 \times \Phi_2 \times \Phi_{12} \equiv \dot{H}_G \times \theta_G \times \gamma_G \times \dot{P}$	4
Γ_7 : Errors in selecting (or variations of) commanded rate of descent, flare start altitude (together with elevator-up increment), and commanded glide slope before touchdown	$\Phi_9 \times (\Phi_{13} + \Phi_{14}) \times \Phi_{15} \equiv \dot{H}_G \times (H_{FL} + \Delta\delta_e) \times \dot{H}_{G1}$	4

Note. See Table 9 for definitions of Φ_i .

Situational trees

In the presented study, a set of nine multifactor situational trees, $\{\mathfrak{S}_1, \dots, \mathfrak{S}_9\}$, has been designed for demonstration (Table 11). The subset $\{\mathfrak{S}_1, \mathfrak{S}_2, \mathfrak{S}_3\}$ relates to takeoff and initial climb, the tree \mathfrak{S}_4 exemplifies level flight followed by climb or descent, the subset $\{\mathfrak{S}_5, \dots, \mathfrak{S}_8\}$ relates to landing approach and go-around, and the tree \mathfrak{S}_9 describes the landing approach, landing and ground-roll phases of flight. Note that these hypothetical compositions represent complex operational domains of flight with two to six demanding factors involved.

Table 11 – Situational trees, $\Omega(\mathfrak{S})$

#	Symbol and name	Operational domain ‘design formula’	$N(\Phi)$
1	$S_1\Gamma_1$: Normal takeoff and initial climb. Errors in selecting (or variations of) commanded flight path and bank angles	$\Phi_1 \times \Phi_2$	2
2	$S_2\Gamma_1$: Continued takeoff and initial climb, with left-hand engine out during ground-roll. Errors in selecting (or variations of) commanded flight path and bank angles	$\Phi_{10} + (\Phi_1 \times \Phi_2)$	3
3	$S_3\Gamma_2$: Continued takeoff and initial climb, with left-hand engine out during ground-roll, in wet runway and cross wind conditions. Variations of wheels-runway adhesion factor, cross wind velocity, and commanded flight path angle	$\Phi_{10} + (\Phi_3 \times \Phi_4 \times \Phi_1)$	4
4	$S_4\Gamma_1$: Level flight followed by climb or descent. Errors in selecting (or variations of) commanded flight path and bank angles	$\Phi_1 \times \Phi_2$	2
5	$S_5\Gamma_3$: Landing approach and go-around in wind shear conditions. Errors in selecting (or variations of) go-around thrust rating, and commanded flight path and bank angles	$\Phi_6 + (\Phi_5 \times \Phi_1 \times \Phi_2)$	4
6	$S_6\Gamma_4$: Landing approach and go-around in wind shear conditions with left-hand engine out. Variations of wind shear intensity, and commanded flight path and bank angles	$\Phi_{11} + (\Phi_6 \times \Phi_1 \times \Phi_2)$	4
7	$S_6\Gamma_5$: Landing approach and go-around in wind shear conditions with left-hand engine out. Errors in selecting (or variations of) go-around thrust increase delay, commanded	$\Phi_6 + \Phi_{11} + (\Phi_8 \times \Phi_1 \times \Phi_7)$	5

SIMULATION RESULTS

Experiment statistics

The key design parameters of the M&S experiment and virtual flight test statistics are summarized in Table 13. For each operational factor Φ_l , $\Phi_l \in \Omega(\Phi)$, a sweep range is set to $\{x_{\min}, x_{\min} + \Delta x, x_{\min} + 2 \cdot \Delta x, \dots, x_{\max}\}$. The way, in which operational factors are combined (dependent or independent), is determined by the corresponding operational hypothesis formula (see Table 11) and a set of logical check conditions, which control the tree growth process during simulation. The length of each flight path-branch from \mathfrak{Z}_n measured in seconds (ΔT) is shown here too, together with the total number of the branches ($N(F)$), which constitute \mathfrak{Z}_n , and the total virtual flight test time measured in hours (T_{Σ}) accumulated in \mathfrak{Z}_n . Note that the total virtual flight test time includes only the 'net' duration of a flight situation from t_s to t^* .

Table 13 – Experiment design parameters and statistics of situational trees, $\Omega(\mathfrak{Z})$

\mathfrak{Z}_n		Operational factor, scenario element and attribute		Operational factor sweep range definition				Resulting tree statistics			
n	$S_i \Gamma_j$	Φ_l	ε	x	x_{\min}	x_{\max}	Δx	U	$\Delta T, s$	$N(F)$	T_{Σ}, hrs
1	$S_1 \Gamma_1$	Φ_1	O_2	θ_G	2	16	1	°	60	225	3.75
		Φ_2	O_3	γ_G	-42	42	6	°			
2	$S_2 \Gamma_1$	Φ_{10}	F_1	δ_{T2}	-5	-	-	%	60	90	1.5
		Φ_1	O_2	θ_G	2	7	1	°			
		Φ_2	O_3	γ_G	-42	42	6	°			
3	$S_3 \Gamma_2$	Φ_{10}	F_1	δ_{T2}	0	-	-	%	60	260	4.33
		Φ_3	Y_1	μ_D	0.2	0.6	0.1	-			
		Φ_4	W_1	$W_{y\bar{g}}$	-18	18	3	m/s			
		Φ_1	O_2	θ_G	2	5	1	°			
4	$S_4 \Gamma_1$	Φ_1	O_9	θ_G	-12	16	2	°	80	195	4.33
		Φ_2	O_3	γ_G	-45	45	7.5	°			
5	$S_5 \Gamma_3$	Φ_6	W_2	k_W	1	-	-	-	70	234	4.55
		Φ_5	P_1	P_{GA}	60	100	20	%			
		Φ_1	O_2	θ_G	4	14	2	°			
		Φ_2	O_3	γ_G	-42	42	7	°			
6	$S_6 \Gamma_4$	Φ_{11}	F_1	δ_{T2}	-5	-	-	%	80	450	10
		Φ_6	W_2	k_W	0.25	1.5	0.25	-			
		Φ_1	O_2	θ_G	1	7	1.5	°			
		Φ_2	O_3	γ_G	-42	42	6	°			
7	$S_6 \Gamma_5$	Φ_6	W_2	k_W	1	-	-	-	80	264	5.87
		Φ_{11}	F_1	δ_{T2}	-5	-	-	%			
		Φ_8	P_1	$\tau(P_{\max})$	0	10	1	s			
		Φ_1	O_2	θ_G	2	5	1	°			
		Φ_7	P_4	$\tau(\delta_{\bar{F}})$	0	10	2	s			
		Φ_1	O_2	θ_G	0.5	6.5	1.5	°			
8	$S_6 \Gamma_6$	Φ_6	W_2	k_W	1	-	-	-	80	450	10
		Φ_{11}	F_1	δ_{T2}	-5	-	-	%			
		Φ_9	O_{10}	\dot{H}_G	-3	-7	-2	m/s			
		Φ_1	O_2	θ_G	0.5	6.5	1.5	°			
		Φ_2	O_3	γ_G	-42	42	6	°			

flight path angle and flaps-up delay			
8	$S_6 \Gamma_6$: Landing approach and go-around in wind shear conditions with left-hand engine out. Errors in selecting (or variations of) commanded rate of descent, commanded flight path and bank angles, and right-hand engine thrust increase rate in climb	$\Phi_6 + \Phi_{11} + (\Phi_9 \times \Phi_1 \times \Phi_2 \times \Phi_{12})$	6
9	$S_7 \Gamma_7$: Landing approach, landing and ground-roll. Errors in selecting (or variations of) commanded rate of descent, flare start altitude (together with elevator-up increment), and commanded glide slope before touchdown	$\Phi_9 \times (\Phi_{13} + \Phi_{14}) \times \Phi_{15}$	4
Note. See Tables 2 and 9 for definitions of and S_i and Φ_j .			

Fuzzy constraints

In the presented study, 19 fuzzy constraints have been defined to measure the compatibility of selected 14 system variables with the operational constraints for each flight F_i from each tree \mathfrak{Z}_j in M&S experiments, $i \in N(F|\mathfrak{Z}_j)$, $\mathfrak{Z}_j \in \Omega(\mathfrak{Z})$. An example specification of the fuzzy constraints for the takeoff scenarios $\{S_1, S_2, S_3\}$, is shown in Table 12. Note that four variables $\{\delta_w, \alpha, \vartheta, IAS\}$ have a pair of definitions of the operational constraints each – depending on the aircraft aerodynamic configuration (flaps extended or retracted) and takeoff segment (ground-roll or airborne) – set up by corresponding events E_s and E^* .

Table 12 – Fuzzy constraints, $\Omega(C)$

Event		Characteristic points of fuzzy set-constraint carrier						Variable	
E_s	E^*	$x_{\rho 1}$	a	b	c	d	$x_{\rho 2}$	x	U
E_1	E_{99}	-	-28	-20	20	28	-	$\delta_{\bar{F}}$	°
E_1	E_{99}	-	-23	-15	10	18	-	$\delta_{\bar{a}}$	°
E_1	E_{99}	-	-23	-19	9	13	-	$\delta_{\bar{c}}$	°
E_1	E_6	-	0	0.9	1.1	2	-	δ_w	-
E_6	E_{99}	-	-1	-0.1	0.1	1	-		
E_1	E_8	-10	-2.5	0	10	20	25	α	°
E_8	E_{99}	-10	-2.5	0	8	13	18		
E_5	E_{99}	-25	-7	-4.5	15	20	-	\dot{H}	m/s
E_1	E_5	-16	-6	-4	4	6	16	ϑ	°
E_5	E_{99}	-40	-10	-5	17.5	25	55		
E_1	E_5	-30	-7.5	-2.5	2.5	7.5	30	γ	°
E_5	E_{99}	-75	-50	-25	25	50	75		
E_1	E_5	-350	-100	0	1500	2000	2250	N	m
E_1	E_5	-80	-50	-25	25	50	80	E	
E_1	E_5	-30	-10	-5	5	10	30	\dot{E}	m/s
E_1	E_{99}	-2.5	0.25	0.5	1.5	1.75	3.75	n_z	-
E_1	E_{99}	45	-15	-10	10	15	45	β	°
E_1	E_8	-	160	190	360	400	600	IAS	km/h
E_8	E_{99}	-	190	220	450	480	600		

Note. See Table 1 for definitions of E_i . Fuzzy constraints $C(x)$ correspond to scenario S_i . $x \subset x$. $x_{\rho 1} < a < b < c < d < x_{\rho 2}$ – see Figure 2. The color coded bars above indicate main safety sub-regions of the definition domain for each monitored variable.

		Φ_{12}	P_1	\dot{P}	1	0.2	-0.8	-			
9	$S_7 \cdot \Gamma_7$	Φ_9	O_{10}	\dot{H}_G	-6	-3	0.5	m/s	120	147	4.9
		Φ_{13}	E_{21}	H_{FL}	7	13	1	m			
		Φ_{14}	P_2	$\Delta \delta_c$	-12	-6	1	°			
		Φ_{15}	O_{11}	\dot{H}_{G1}	-0.3	-0.1	0.1	m/s			
Overall virtual flight test time, hrs:											49.24

3D view of selected trees

Figure 8 depicts a three-dimensional view of four selected situational trees in earth frames. In this illustration, black background is utilized to help better visualize a very high density and varying flight safety spectra colors observed in each tree's crown. 'Flight' (branch) codes are typed in brown color at branch ends. The nodes of high-order sub-tree branching are clearly seen for the trees \mathfrak{S}_5 and \mathfrak{S}_8 , too.

Integral safety spectra maps

Two families of the integral safety spectra Σ_k and flight safety categories ξ_k constructed for the normal and continued takeoff domains, $\mathfrak{S}_1 \equiv S_1 \cdot \Gamma_1$ ($k = 1, \dots, 225$) and $\mathfrak{S}_2 \equiv S_2 \cdot \Gamma_1$ ($k = 1, \dots, 90$), are shown in Figure 9. Two families of the integral safety spectra Σ_k , which correspond to the continued takeoff domain $\mathfrak{S}_3 \equiv S_3 \cdot \Gamma_2$ ($k = 1, \dots, 260$) and the level flight domain $\mathfrak{S}_4 \equiv S_4 \cdot \Gamma_1$ ($k = 1, \dots, 195$), are also shown in Figure 10. Four families of the integral safety spectra Σ_k for the landing approach and go-around domains $\mathfrak{S}_5 \equiv S_5 \cdot \Gamma_3$ ($k = 1, \dots, 234$), $\mathfrak{S}_6 \equiv S_6 \cdot \Gamma_4$ ($k = 1, \dots, 450$), $\mathfrak{S}_7 \equiv S_6 \cdot \Gamma_5$ ($k = 1, \dots, 264$) and $\mathfrak{S}_8 \equiv S_6 \cdot \Gamma_6$ ($k = 1, \dots, 450$) constructed under various multifactor conditions are exhibited in Figures 11, 12, 13 and 15, respectively. Finally, a family of the the integral safety spectra Σ_k constructed for the landing approach and landing domain $\mathfrak{S}_9 \equiv S_7 \cdot \Gamma_7$ ($k = 1, \dots, 147$) is shown in Figure 14.

Safety Windows

Examples of the safety windows constructed for selected operational sub-domains of flight $\mathfrak{S}_1 \equiv S_1 \cdot \Gamma_1$, $\mathfrak{S}_2 \equiv S_2 \cdot \Gamma_1$, $\mathfrak{S}_6 \equiv S_6 \cdot \Gamma_4$ and $\mathfrak{S}_7 \equiv S_6 \cdot \Gamma_5$ are depicted in Figure 16. A more detailed introduction to the concept, implementation and examples of the safety window technique can be found in [11, 12].

DISCUSSION

Following is a brief discussion of the main results obtained from M&S experiments.

Research performance and statistics

The system model includes a human pilot model (a 'silicon pilot'). It means that the M&S process is fully autonomous and runs without an external research pilot or engineer in the

flight control simulation loop. As a result, the speed of complex flight domain exploration using the model can be much faster than real time simulations. At present, it falls in the range of $1:(20 \cdot N) \dots 1:(100 \cdot N)$, depending on the processor performance, where N is the number of computers used for M&S. For example, if $N = 1$ (a single standard computer, with a 2.16 GHz dual CPU and 2 Gb RAM) then the speed of simulation is within the range of $1:20 \dots 1:75$ depending on the output M&S data flow requested and the 'richness' of the aircraft's parametric definition database.

The amount of manual labor in the M&S process is therefore minimal. There are still several time-consuming tasks. The major one is the design of a 'parametric definition' database for the vehicle of interest. The next manual task is to specify the operational factors and their composite for virtual testing in a situational tree, and to define the structure of the M&S output data flows and the nomenclature of desired knowledge maps. Normally, baseline flight scenarios are constructed and debugged easily.

The remaining (major) part of the M&S based research process runs automatically. The following M&S functions are fully automatic – in addition to fast-time flight simulation: parametric variation of a baseline flight scenario and operational factors according to a given composition $S \cdot \Gamma$, tree growth management (initialization, growth, growth control, marking, pre-processing, storing, etc.), construction of knowledge maps, general M&S experimentation control.

The overall virtual flight test time accumulated in the 'forest' $\Omega(\mathfrak{S})$ of situational trees, $\Omega(\mathfrak{S}) = \{\mathfrak{S}_1, \dots, \mathfrak{S}_9\}$, is equal to 49.24 hours (see Table 13). This corresponds to the research cycle of the construction and examination of nine situational trees with the parameters defined in Tables 2-13. The net duration of the M&S experiments carried out to build the set $\Omega(\mathfrak{S})$ is about 2 hours. The resources required to obtain the above described results are: the system model, a computer and a researcher. The presented virtual flight test methodology helps save time, budget and other resources for advanced safety research, with a substantial ($10^2 \dots 10^3$ times) increase in the volume of the system level predictive knowledge obtained from M&S of complex operational domains of flight.

Situational trees

It follows from Figure 8 that two- or three-dimensional views of a situational tree displayed in an appropriate coordinate system can be used for a high level mapping and topology analysis of complex operational domains of flight (with additional options for color coding, event marking and other processing of its branches). For instance, Figure 8 clearly indicates the location of a tree's branching nodes, state space regions with dominating (stable) or varying (unstable) safety colors in integral safety spectra, potential accident precursors

(near-hazard circumstances), as well as catastrophic and recovery branches.

This kind of maps are also potentially useful as a knowledge base and virtual decision-making environment for research into intelligent ‘operator – vehicle’ interface systems. Using haptic devices, the operator can virtually navigate inside a ‘forest’ of situational trees in desired directions, back and forth in time, and explore multifactor operational space, e.g.: add or eliminate controllable factors (accident precursors or recovery processes), vary other key scenario elements, look for a best and worst sub-domain of branches in terms of safety or mission effectiveness, etc.

Integral safety spectra and safety windows

Figures 9-16 demonstrate that a family of the integral safety spectra and safety windows constructed for a complex operational sub-domain of flight is a valuable source of both quantitative and qualitative knowledge about anomalous (catastrophic), unsafe, interim and safe options of flight under multifactor conditions. In particular, these knowledge maps help identify prohibited combinations of operational factors and flight modes (evident hazards), as well as possible accident precursors (less severe operational multifactor combinations and flight modes), which are typically adjacent to a hazard.

Integral safety spectra and safety window maps can also be useful to help implement the ICAO recommendations on risk management in flight operations, namely hazard identification, risk assessment and risk mitigation [13]. For examples, the relationship between operational composites and characteristic safety cases in the system behavior (‘maximum safety’, ‘standard safety’, ‘satisfactory safe’, ‘conditionally safe’, ‘accident precursor’, and ‘dangerous’) for the situational tree $S_1 \cdot \Gamma_1$ is shown in Table 14 – see also Figure 16 (a). Some other potential hazards and accident precursors are exemplified in Table 15 for the scenario subset $\{S_2, S_3, S_4, S_6\}$ – see also Figure 16 (b, c).

Table 14 – Characteristic safety cases and operational factor composites in situational tree $S_1 \cdot \Gamma_1$

Category ξ_i	Situation segment	Combinations of commanded flight path and bank angles		Case characteristic
		Φ_1/θ_G	Φ_2/γ_G	
I	Initial climb	+8° ... +9°	-12° ... +12°	Maximum safety
I	Initial climb	+5° ... +12°	-30° ... +30°	Standard safety
II-a	Initial climb	See Figure 16 (a)	- See Figure 16 (a)	Satisfactory safety
II-b	Initial climb	See Figure 16 (a)	See Figure 16 (a)	Conditionally safe
III	Initial climb	See Figure 16 (a)	See Figure 16 (a)	Accident precursor
IV	Initial climb	+16° +15° +15° +14°	∇ -42° ... -30° +24° ... +42° 42°	Dangerous

V	Initial climb	-	-	Catastrophic
----------	---------------	---	---	--------------

Table 15 – Potential hazard and accident precursor examples for selected operational hypotheses

Fight scenario	Hazards	Accident precursors
S₂ : Continued takeoff and initial climb, with left-hand engine out during ground-roll.	Initial climb options with flight path angle $\leq 2^\circ \dots 3^\circ$. Flight maneuvers with left bank angle $\leq -42^\circ \dots -24^\circ$. Initial climb with flight path angles $6^\circ \dots 7^\circ$ and bank angle $-30^\circ \dots -12^\circ$.	Initial climb options with flight path angles $5^\circ \dots 6^\circ$ and bank angles varying within $-24^\circ \dots +30^\circ$. See also Figure 16(b).
S₃ : Continued takeoff and initial climb, with left-hand engine out during ground-roll, in wet runway and cross wind conditions.	Initial climb options with cross wind velocity $-6 \dots -18$ m/s and flight path angle $> 4^\circ$. Other hazards – see Figure 10 (a).	Initial climb options with cross wind velocity of $-9 \dots -18$ m/s and flight path angle $> 4^\circ$. Other hazardous cases – see Figure 10 (a).
S₄ : Level flight followed by climb or descent.	All descent options with flight path angle $\leq 12^\circ$ and any bank angle. Descent options with bank angle $\geq 45^\circ $ and flight path angles $\leq -10^\circ$.	Descent with flight path angles $-9^\circ \dots -10^\circ$ and any bank. Climb with flight path angle $\geq 12^\circ$ and bank $\geq 37^\circ $. Climb options with flight path angle $\geq 14^\circ$ and bank $\geq 22^\circ \dots 37^\circ $. Climb options with flight path angle $\geq 16^\circ$ and any bank.
S₆ : Landing approach and go-around in wind shear conditions with left-hand engine out.	Thrust increase delay ≥ 3 s and flight path angle $\geq 5^\circ$. Thrust increase delay ≥ 7 s and flight path angle 4° . Flaps-up delay does not matter.	Thrust increase delay $2 \dots 3$ s and flight path angle $\geq 5^\circ$. Thrust increase delay $4 \dots 6$ s and flight path angle 4° . Flaps-up delay does matter. See Figure 16 (c).

CONCLUSIONS

The developed methodology makes it possible to automate the tasks of planning, exploration, analysis and mapping of a broad set of realistic multifactor flight scenarios in autonomous fast-time simulation experiments using the system model. This technique is expedient to use for studying in advance complex or unknown operational domains of flight, when the system state can go close to or beyond operational constraints.

The list of these problems includes, but is not limited to, the following: research into new flight maneuvers and innovative aircraft configurations, rehearsal of multifactor flight test scenarios and complex aerobatic sequences; development of control tactics for rough terrain or urban obstacles avoidance, automatic control in tight formation flight; research into recovery techniques from unusual spatial attitudes, spin or stall; development of built-in safety/backup systems for the prevention of ‘9/11’ type scenarios; independent analysis of disputed accidents and accidents occurred under unknown or highly complex operational conditions; verification and validation of manual control tactics and automatic flight control algorithms under multifactor conditions in design;

theoretical pilot training in multifactor situations; research into robotic aircraft swarm flight control. The system level safety knowledge bases generated by means of the model can be potentially useful for the following categories of specialists: aircraft designers, flight test pilots/test engineers, regulators, educators/ instructors, investigators, and line pilots.

REFERENCES

1. D.A. Pospelov, Situational Control. Theory and Practice, M., Nauka, 1986, 288 pp. (In Russian).
2. VATES (Virtual Autonomous Test and Evaluation Simulator) – software tool for studying ‘pilot (automaton) – aircraft – operational environment’ system behavior in complex (multifactor) flight situations, INTELONICS Ltd., Software Registration Certificate # 2007613256, Moscow, 2007. (In Russian).
3. N. Wirth, Programming in Oberon, 2004, 64 pp. <http://www-old.oberon.ethz.ch/WirthPubl/ProgInOberon.pdf>. Accessed on 21 March 2011.
4. Richard E. McFarland, A Standard Kinematic Model for Flight Simulation at NASA-Ames, NASA CR-2497, January 1975, 53 pp.
5. E. Bruce Jackson, Manual for a workstation-based generic flight simulation program (LaRCsim), version 1.4, NASA TM 110164, 1995, 27 pp.
6. P.G. Thomasson, Flight Dynamics Simulation, *Lecture Notes*, College of Aeronautics, Cranfield University, UK, 1993.
7. M.V. Cook, Flight Dynamics Principles, Arnold, 1997, 379 pp.
8. Malcolm J. Abzug, Computational Flight Dynamics, AIAA, 1998, 470 pp.
9. S.A. Gorbatenko, et al., Flight Mechanics, M., Mashinostroyeniye, 1969, 420 pp. (In Russian).
10. L.A. Zadeh, Toward a theory of fuzzy information granulation and its centrality in human reasoning and fuzzy logic, *Fuzzy sets and systems*, vol. 90, 1997, pp. 111-127.
11. I.Y. Burdun, The Intelligent Situational Awareness and Forecasting Environment (The S.A.F.E. Concept): A Case Study (Paper 981223), *Proceedings of the SAE Advances in Flight Safety Conference and Exhibition, April 6-8, 1998, Daytona Beach, FL (P-321)*, SAE Aerospace, USA, 1998, pp. 131-144.
12. I.Y. Burdun, Safety Windows: Knowledge Maps for Accident Prediction and Prevention in Multifactor Flight Situations, *27th Congress of the International Council of Aeronautical Sciences (ICAS 2010), 19-24 September 2010, Nice*, ICAS, France, 2010, 15 pp.
13. Safety Management Manual (SMM), Doc. 9859, ICAO, 2006.

CONTACT INFORMATION

Dr. Ivan Y. Burdun, Chief Scientist, INTELONICS Ltd., Novosibirsk, Russia. E-mail: info@intelonics.com. Phone (cell.): +7 (961) 877 32 89. Internet: www.intelonics.com.

DEFINITIONS/ABBREVIATIONS

MAIN SYMBOLS

\dot{x}	Rate of change: $\frac{dx}{dt}$, $x \in \{\beta, \gamma, \theta, \psi, H, E, \dot{H}, \dots\}$	■	Potential danger (accident precursor)
α	Angle of attack	■	Standard safety (normal operation)
γ	Bank angle	■	Maximum safety or mission effectiveness (optimal mode)
\emptyset	Empty set	■	Satisfactory safety (pilot attention required)
\equiv	Equivalent	■	Almost standard safety
θ	Flight path angle	Δ	Time increment for ‘flight’ data file recording
ε	Flight scenario element, $\varepsilon \in \{I, E, T, O, P, F, W, Y, \dots\}$	$\Delta\delta$	Flight control δ increment
ψ	Heading angle	$\Omega(\dots)$	Set of elements ...
\square	Logical relation, $\square \in \{>, \geq, <, \leq, =, \neq, \approx, \neg\}$	$\xi(t)$	Situation safety color at time instant t , $\xi(t) \in \pi$
ϑ	Pitch angle	$\tau(\Pi)$	Delay of starting process Π with respect to its source event
β	Sideslip angle	$\xi_1 < \xi_2$	Safety color ξ_1 is hotter than safety color ξ_2
μ	Wheels-runway adhesion factor	ΔT	‘Flight’ duration (situational tree branch ‘length’)
δ	Flight control, flight control deflection angle	Δx	Operational factor variable value increment
ζ	Engine ‘health’ state variable: $\zeta = 1$ (operative), $\zeta = 0$ (out)	$[\dots]$	Range of values ...
\mathfrak{S}	Situational tree	$\{\dots\}$	Set of values ...
\times	Dependent combination of operational factors	\parallel	Geometric concatenation operation
π	Safety palette, $\pi \in \{\text{blue}, \text{green}, \text{yellow}, \text{red}, \text{black}, \text{grey}, \dots\}$	$+$	Independent combination of operational factors
Σ	Integral safety spectrum	A	Right part of event recognition criterion
\wedge	Logical AND	A	‘Atmospheric state’ type process
\vee	Logical OR	$A \rightarrow B$	Changing from A to B
\cdot	‘Baseline scenario – operational hypothesis’ composition	a, b, c, d	Characteristic points of a fuzzy set-constraint carrier
∇	Logical link, $\nabla \in \{\wedge, \vee\}$	$A B$	Element A corresponding to B
■	Catastrophe (flight anomaly)	B	‘Automaton functioning’ type process
■	Danger (severe violation of constraints)	C	Fuzzy constraint
		E	East distance (earth frames)

E	Flight event
f	function
F	‘Mechanical malfunction’ type process
F	‘Flight’ (flight simulation experiment data set), $F \in \Omega(F)$
H	Flight altitude
hrs	Hours
I	‘Initial conditions’ type scenario element
I, II, ..., V	Flight safety categories
IAS	Indicated airspeed
km/h	Kilometer per hour
kN	KiloNewton
k_W	Wind shear intensity factor: $\vec{W}_{fact} = k_W \cdot \vec{W}_{baseline}$
L	‘Turbulence’ type process
m	Meter
M&S	Mathematical modeling and computer simulation
m/s	Meter per second
max	‘hottest’ safety color selection operation
N	North distance (earth frames)
N	Number of elements
n	Total number of records in a ‘flight’ file
n	Number of independent branching levels in a tree
N	Number of elements
$N(\Omega)$	Number of elements in set Ω
$N(\dots)$	Number of ... type elements
n_z	Load factor (body frames)
O	‘System state observer’ type process
P	‘Control procedure’ type process
p	Roll rate
P	Thrust
q	Pitch rate
R	Vertical reaction of landing gear strut
r	Yaw rate
S	Baseline [flight situation] scenario
s	Second
s	Vertical displacement of main landing gear strut
S·Γ	Composition of scenario S and operational hypothesis Γ
T	‘Piloting task’ type process
T	Total virtual flight test time accumulated in a tree
t	Flight time
$t(\mathbf{E})$	Event E recognition time instant
U	Physical measurement unit
V	Airspeed
W	‘Wind’ type process
W	Safety window calculation matrix
W	Wind velocity component
w	Safety window’s cell
x	System state [model] variable, $x \in \mathbf{x}$
\mathbf{x}	System state vector
Y	‘Runway surface condition’ type process
y	Main observed variable, $y \in \{\gamma, \theta, \psi, H, \dot{H}, IAS, \dots\}$
y	State observation vector, $y \subset \mathbf{x}$
Γ	Operational hypothesis, $\Gamma \in \Omega(\Gamma)$

Π	Flight process, $\Pi \in \{\mathbf{T}, \mathbf{O}, \mathbf{P}, \mathbf{F}, \mathbf{W}, \mathbf{Y}, \mathbf{A}, \mathbf{L}, \mathbf{B}, \dots\}$
Φ	Numeric value of operational factor
Φ	Operational factor, $\Phi \in \Omega(\Phi)$

SUBSCRIPTS

a	First factor identification number
Σ	Total
*	Start or source [flight event]
0	Baseline scenario related
a	Ailerons
A.BR	Air brakes
b	Second factor identification number
B	Black (for safety color)
D	Decelerometer
e	Elevator
EF	Engine failure
F	Flaps
$f_1(f_2)$	Fuzzy set black-red (red-black) zones separation point
FL	Flare
G, G1	Goal, or commanded value of a state variable
G	Green (for safety color)
GA	Go-around
GR.SP	Ground spoilers
i, j, k	Ordinal number, or identification code
LEO	Left-hand engine out
LG	Landing gear
$LG_{2(3)}$	Right- (left-) hand landing gear
max	Maximum value
min	Minimum value
n	Number of elements, element number
N.W	Nose wheel
r	Rudder
R	Rotation
R	Red (for safety color)
T	Turquoise (for safety color)
T_i	Throttle (engine # i)
W	White or grey (for safety color)
W	Wheels, or with respect to wheels
W.BR	Wheels brakes
x_g, y_g, z_g	X_g, Y_g , or Z_g axis (earth frames)
Y	Yellow (for safety color)
z	Z axis (body frames)

SUPERSCRIPTS

o	Degree
*	Stop or target (flight event, time)
IF	IF-event (event-precondition for other event)
i	Ordinal number, or code, $i = 1, 2, \dots$

APPENDIX

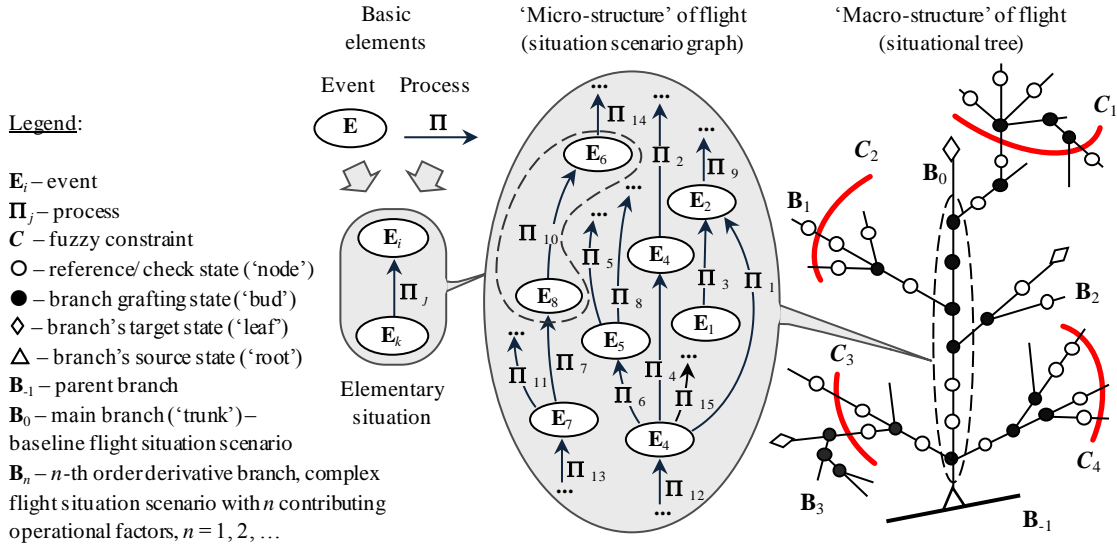


Figure 1 – Two-level memory based knowledge model of complex (multifactor) flight situations domain.

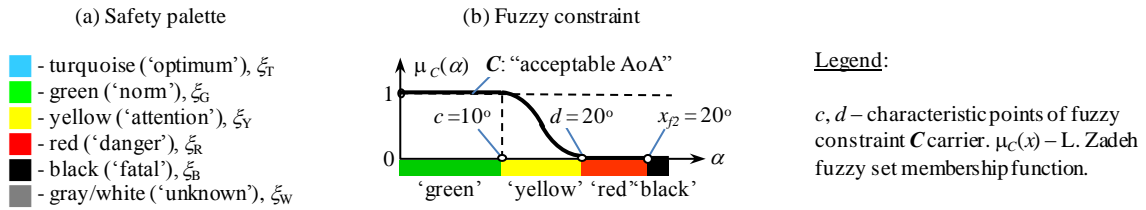


Figure 2 – Safety palette and fuzzy constraint concepts.

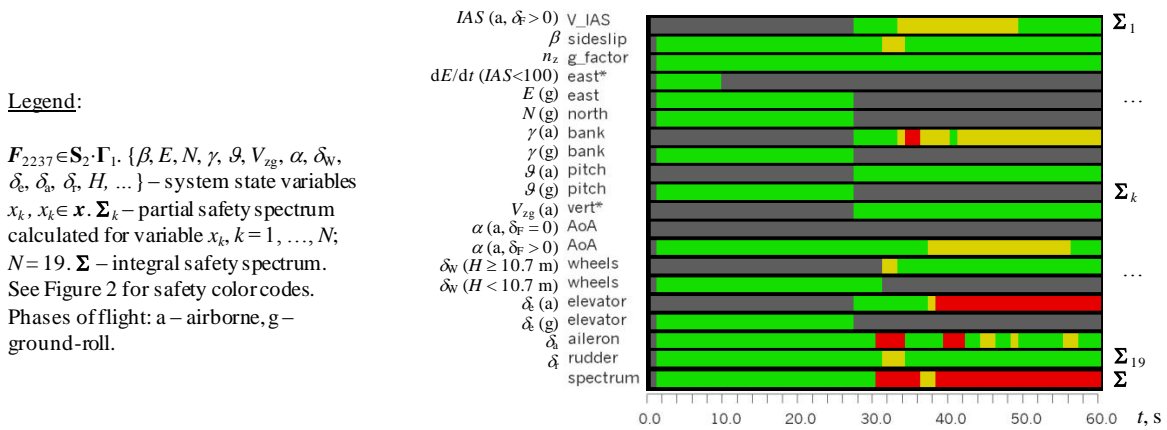


Figure 3 – Safety spectra for flight F_{2237} : 'Continued takeoff and initial climb at commanded flight path angle $\theta_G = 5^\circ$ and commanded bank angle $\gamma_G = -42^\circ$ with left-hand engine out during ground roll'.

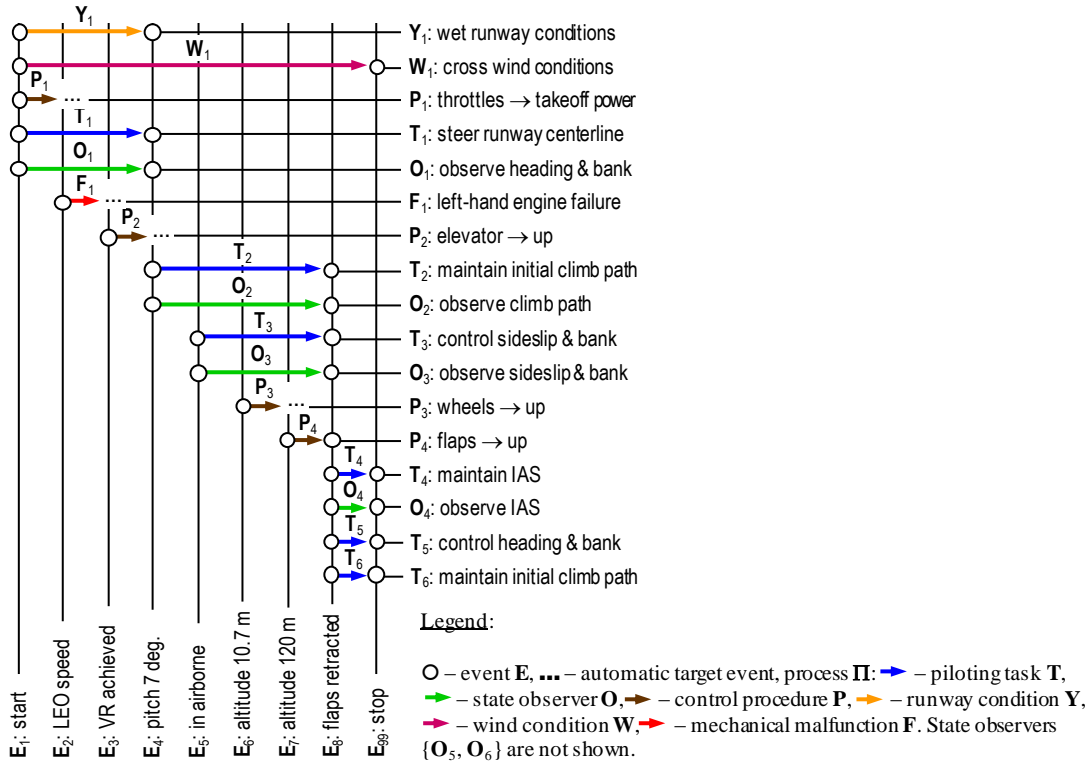


Figure 4 – Baseline scenarios S_1 : ‘Normal takeoff and initial climb’, S_2 : ‘Continued takeoff and initial climb, with left-hand engine out during ground-roll’ and S_3 : ‘Continued takeoff and initial climb, with left-hand engine out during ground-roll, in wet runway and cross wind conditions’ (joint graph).

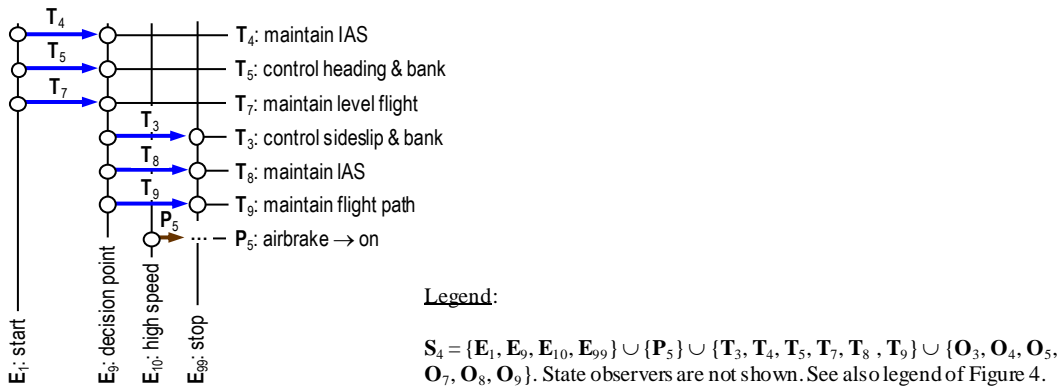


Figure 5 – Baseline scenario S_4 : ‘Level flight followed by climb or descent’.

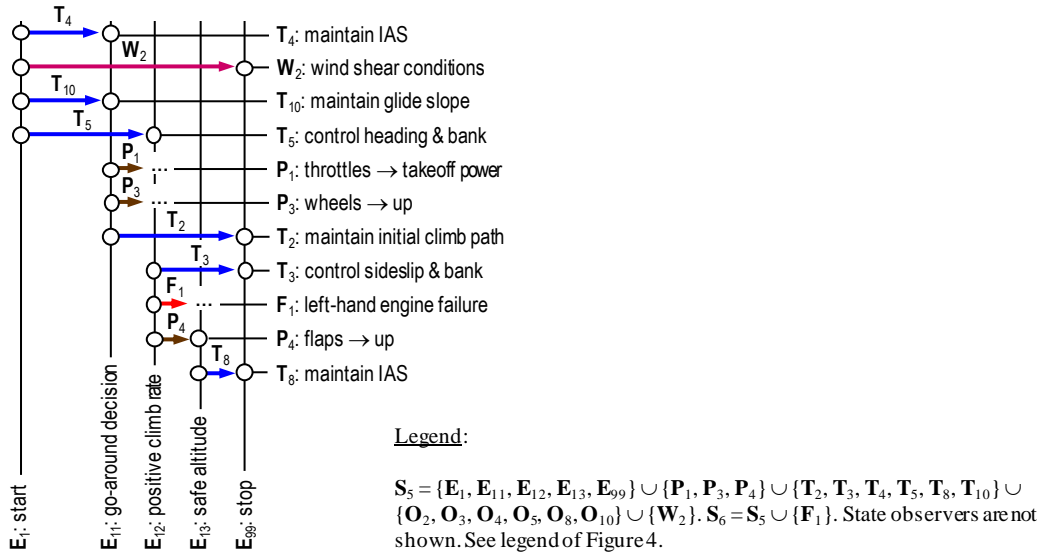


Figure 6 – Baseline scenarios S_5 : ‘Landing approach and go-around in wind shear conditions’ and S_6 : ‘Landing approach and go-around in wind shear conditions with left-hand engine out’ (joint graph).

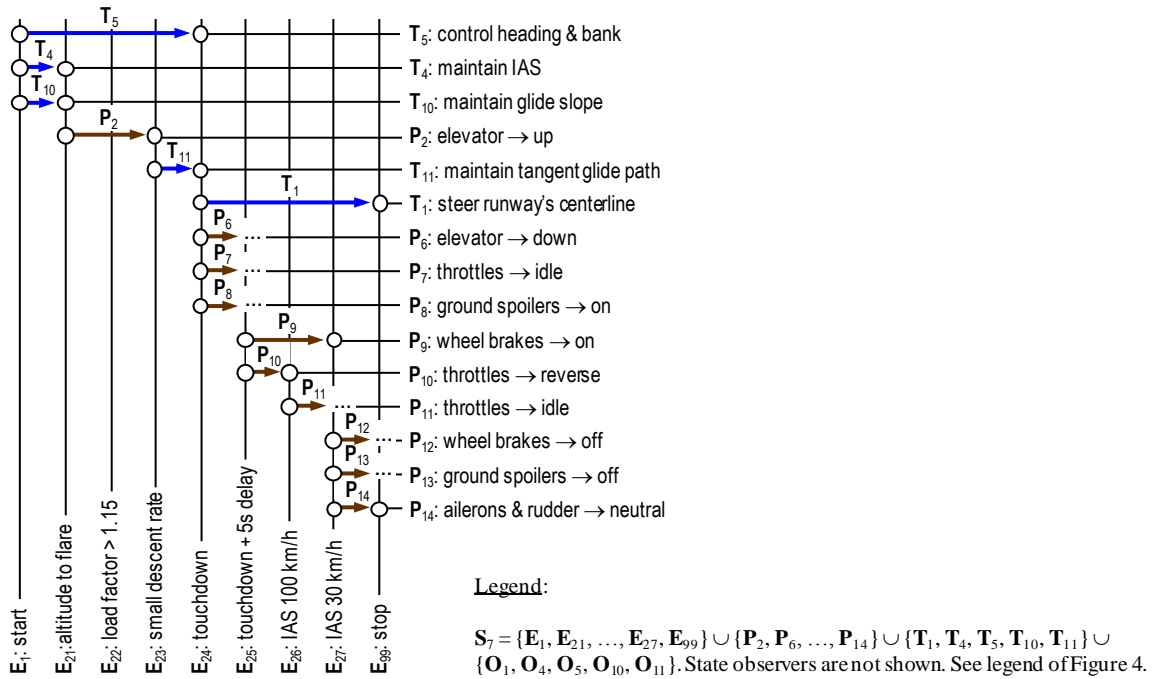
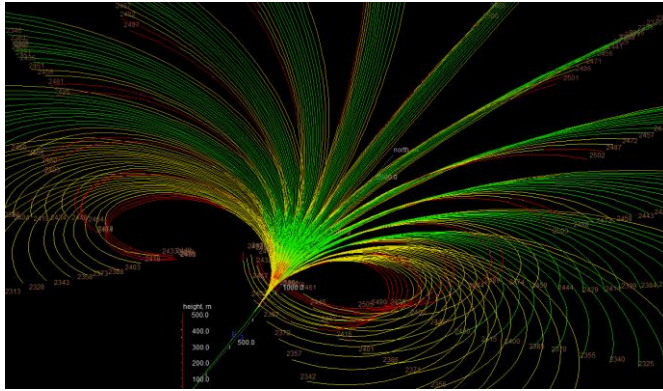


Figure 7 – Baseline scenario S_7 : ‘Landing approach, landing and ground-roll’.

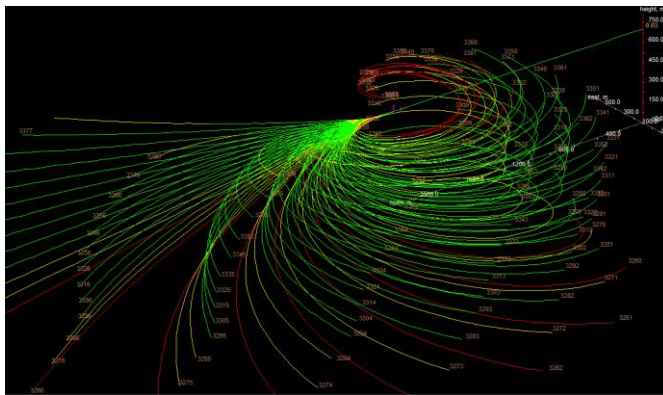
(a) Tree $\mathfrak{S}_1 \equiv \mathbf{S}_1 \cdot \Gamma_1$:

Normal takeoff and initial climb. Errors in selecting (or variations of) commanded flight path and bank angles.



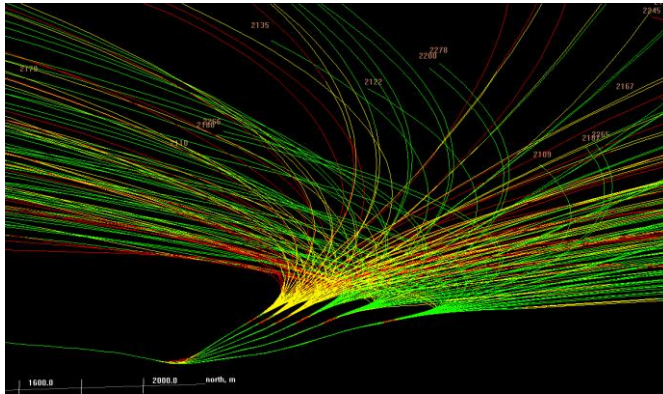
(b) Tree $\mathfrak{S}_4 \equiv \mathbf{S}_4 \cdot \Gamma_1$:

Level flight followed by climb or descent. Errors in selecting (or variations of) commanded flight path and bank angles – only a left-hand sub-tree is shown, i.e. for $\gamma_G \in [-45^\circ; 0]$.



(c) Tree $\mathfrak{S}_5 \equiv \mathbf{S}_5 \cdot \Gamma_3$:

Landing approach and go-around in wind shear conditions. Errors in selecting (or variations of) go-around thrust rating, and commanded flight path and bank angles.



(d) Tree $\mathfrak{S}_8 \equiv \mathbf{S}_6 \cdot \Gamma_6$:

Landing approach and go-around in wind shear conditions with left-hand engine out. Errors in selecting (or variations of) commanded rate of descent, commanded flight path and bank angles, and right-hand engine thrust increase rate in climb.

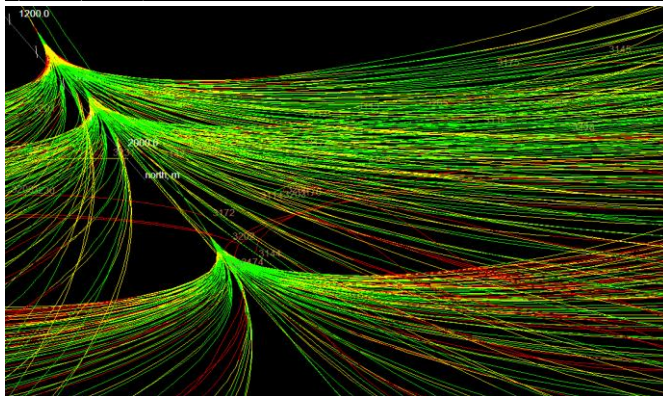
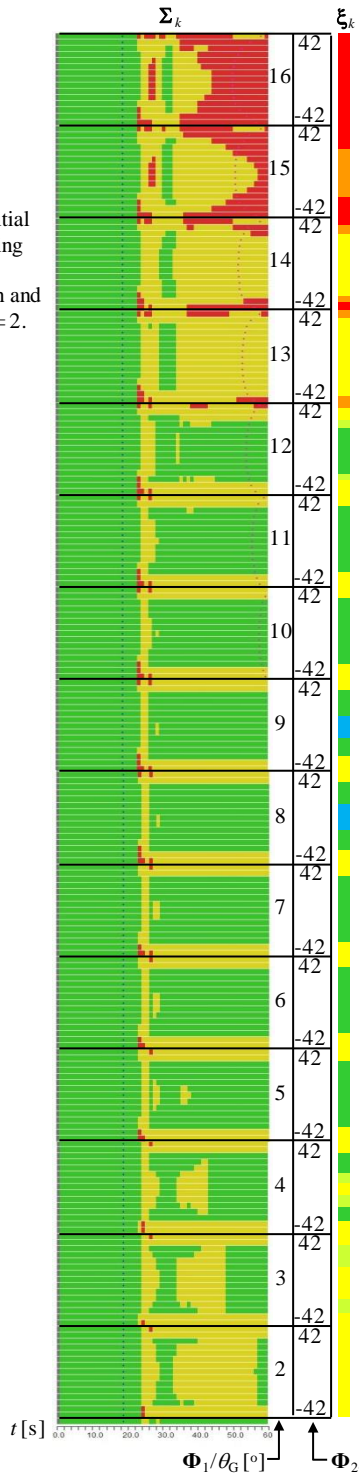


Figure 8 – A three-dimensional view of selected situational trees (branches are colored with integral safety spectra).

(a) Tree $\mathfrak{F}_1 \equiv \mathbf{S}_1 \cdot \Gamma_1$:

Normal takeoff and initial climb. Errors in selecting (or variations of) commanded flight path and bank angles. $N(\Phi|\mathfrak{F}_1) = 2$.



Legend:

See Tables 9-13; t [s] – flight time scale; Σ_k – integral safety spectrum of ‘flight’ F_k , $F_k \in \mathbf{S}_i \cdot \Gamma_1$, $k = 1, \dots, N(\mathbf{S}_i \cdot \Gamma_1)$, $i \in \{1, 2\}$; $\mathfrak{F}_1 \equiv \mathbf{S}_1 \cdot \Gamma_1 = \Phi_1 \times \Phi_2$ or $\mathfrak{F}_1 = \theta_G \times \gamma_G$, $\theta_G \in \{2, 3, \dots, 16\}$ [°], $\gamma_G \in \{-42, -36, \dots, 42\}$ [°], $N(\mathbf{S}_1 \cdot \Gamma_1) = 225$; $\mathfrak{F}_2 \equiv \mathbf{S}_2 \cdot \Gamma_1 = \Phi_{10} + (\Phi_1 \times \Phi_2)$ or $\mathfrak{F}_2 = \delta_{12} + \theta_G \times \gamma_G$, $\delta_{12} = -5\%$ – see Figure 4, $\theta_G \in \{2, 3, \dots, 7\}$ [°], $\gamma_G \in \{-42, -36, \dots, 42\}$ [°], $N(\mathbf{S}_2 \cdot \Gamma_1) = 90$; ξ_k – safety category of F_k , $\xi_k \in \{\text{I, II-a, II-b, III, IV, V}\}$ or $\xi_k \in \{\text{blue, green, yellow, orange, red, black}\}$.

(b) Tree $\mathfrak{F}_2 \equiv \mathbf{S}_2 \cdot \Gamma_1$:

Continued takeoff and initial climb, with left-hand engine out during ground-roll. Errors in selecting (or variations of) commanded flight path and bank angles. $N(\Phi|\mathfrak{F}_2) = 3$.

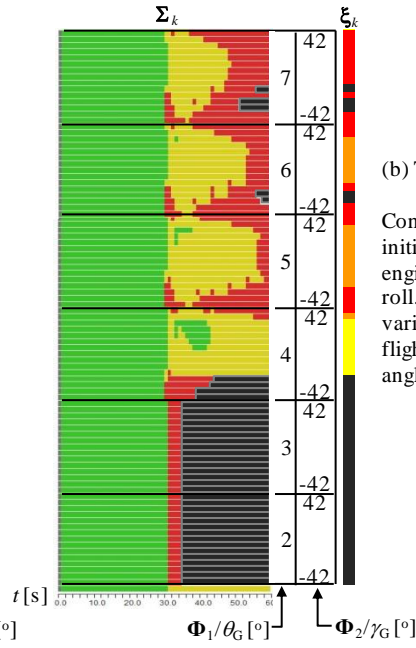


Figure 9 – Integral safety spectra and safety categories for flight domain $\mathfrak{F}_1 \equiv \mathbf{S}_1 \cdot \Gamma_1$: ‘Normal takeoff and initial climb. Errors in selecting (or variations of) commanded flight path (Φ_1) and bank (Φ_2) angles’ and $\mathfrak{F}_2 \equiv \mathbf{S}_2 \cdot \Gamma_1$: ‘Continued takeoff and initial climb, with left-hand engine out (Φ_{10}) during ground-roll. Errors in selecting (or variations of) commanded flight path (Φ_1) and bank (Φ_2) angles’.

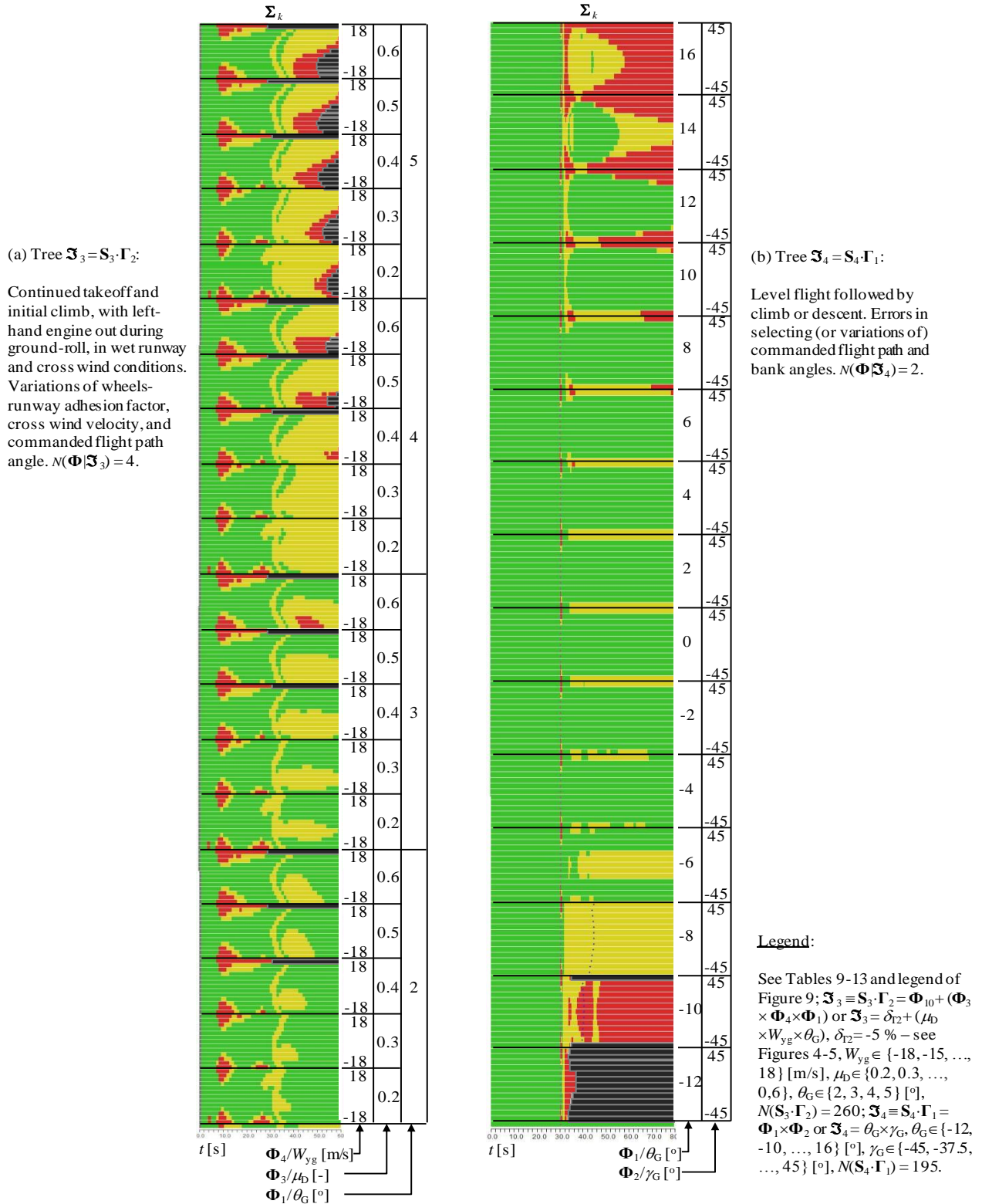


Figure 10 – Integral safety spectra for flight domains $\mathfrak{S}_3 \equiv \mathbf{S}_3 \cdot \Gamma_2$: ‘Continued takeoff and initial climb, with left-hand engine out (Φ_{10}) during ground-roll in wet runway and cross wind conditions. Variations of wheels-runway adhesion factor (Φ_3), cross wind velocity (Φ_4), and commanded flight path angle (Φ_1)’ and $\mathfrak{S}_4 \equiv \mathbf{S}_4 \cdot \Gamma_1$: ‘Level flight followed by climb or descent. Errors in selecting (or variations of) commanded flight path (Φ_1) and bank (Φ_2) angles’.

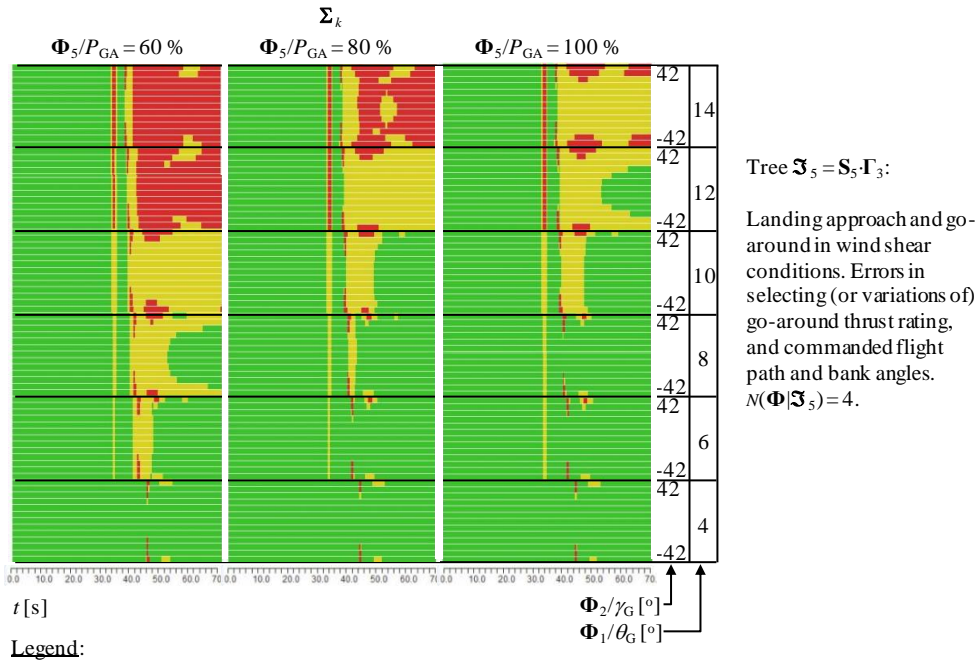


Figure 11 – Integral safety spectra for flight domain $\mathfrak{S}_5 \equiv \mathbf{S}_5 \cdot \Gamma_3$: ‘Landing approach and go-around in wind shear conditions (Φ_6). Errors in selecting (or variations of) go-around thrust rating (Φ_5), and commanded flight path (Φ_1) and bank (Φ_2) angles’.

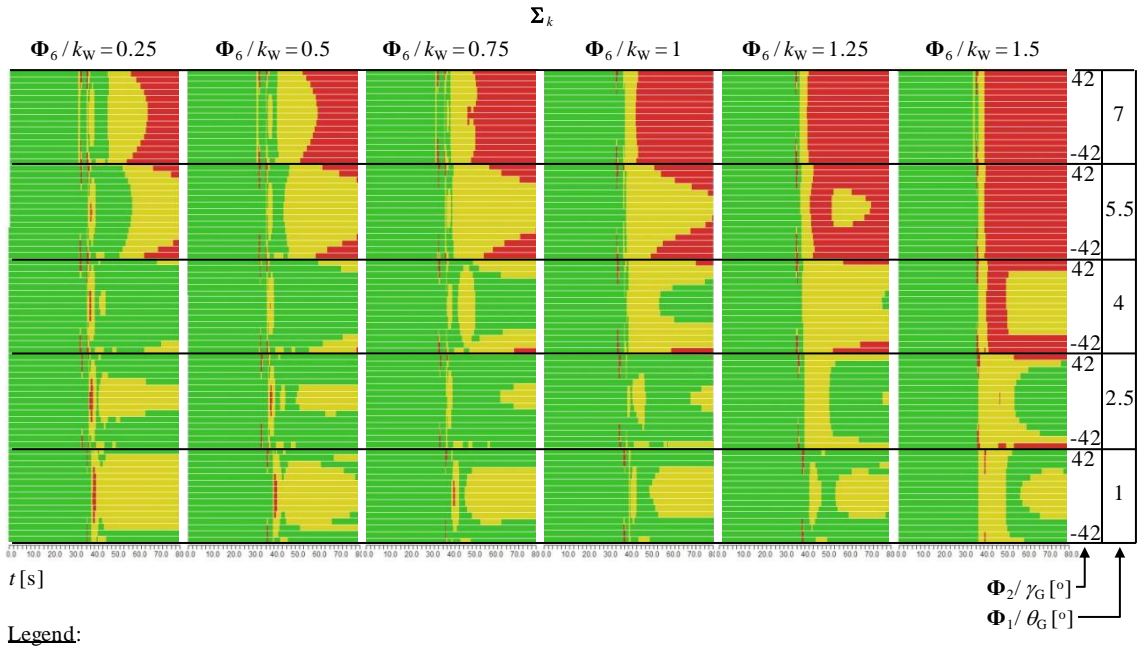
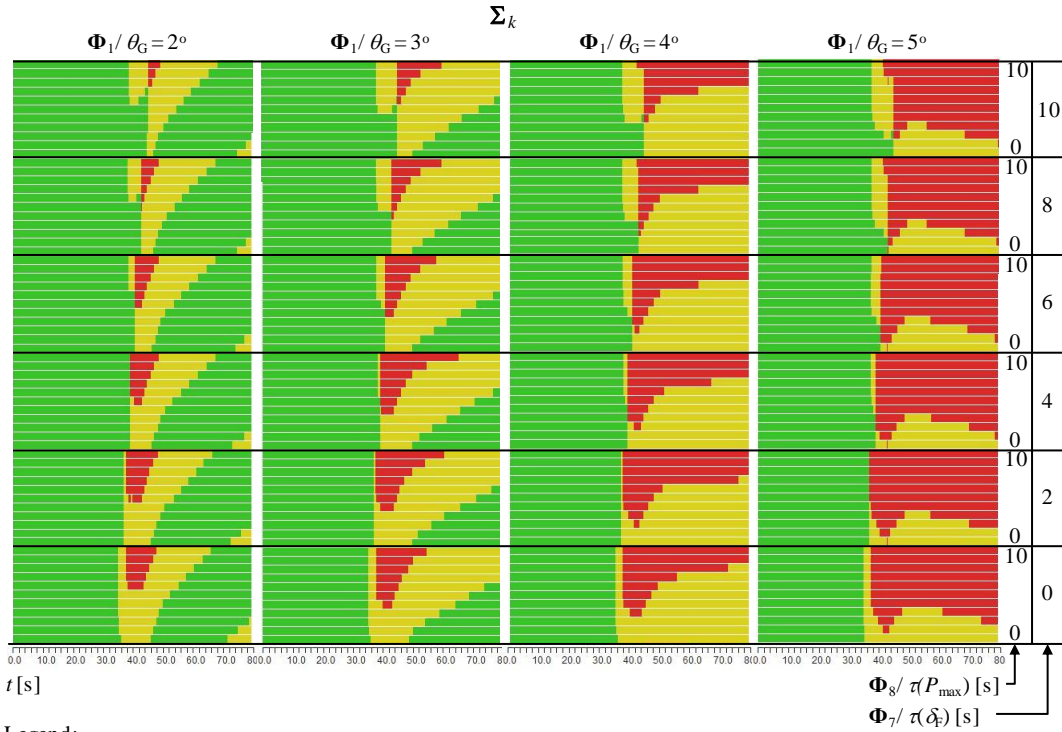


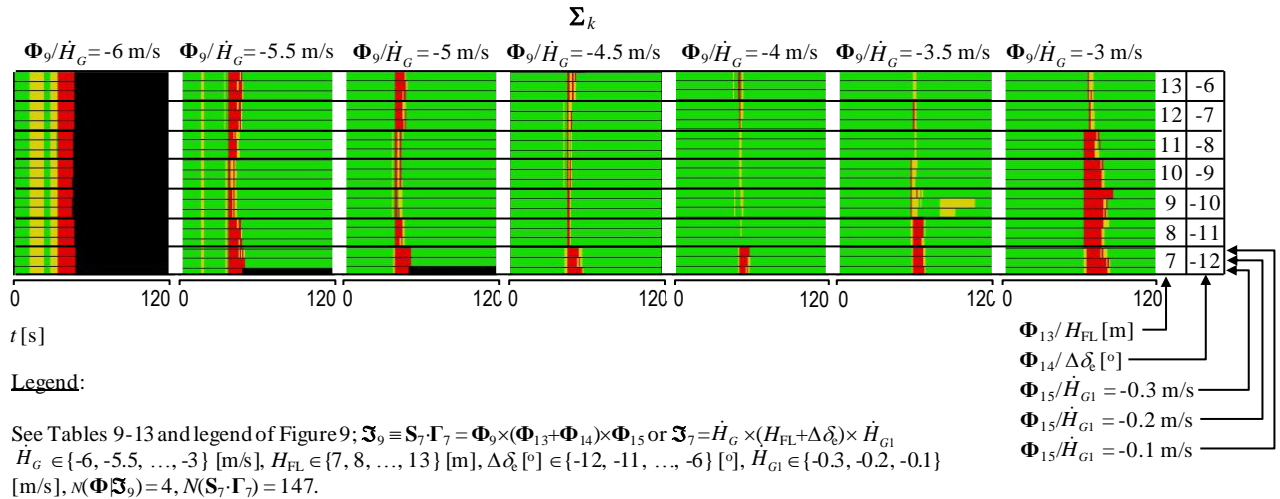
Figure 12 – Integral safety spectra for flight domain $\mathfrak{S}_6 \equiv \mathbf{S}_6 \cdot \Gamma_4$: ‘Landing approach and go-around in wind shear conditions with left-hand engine out (Φ_{11}). Variations of wind shear intensity (Φ_6) and commanded flight path (Φ_1) and bank (Φ_2) angles’.



Legend:

See Tables 9-13 and legend of Figure 9; $\mathfrak{S}_7 \equiv S_6 \cdot \Gamma_5 = \Phi_6 + \Phi_{11} + (\Phi_8 \times \Phi_1 \times \Phi_7)$ or $\mathfrak{S}_7 = k_w + \delta_{12} + (\tau(P_{\max}) \times \theta_G \times \tau(\delta_\phi))$, $k_w = 1$ – see Table 8, $\delta_{12} = -5\%$ – see F_1 in Figure 6, $\tau(P_{\max}) \in \{0, 1, \dots, 10\}$ [s], $\theta_G \in \{2, 3, 4, 5\}$ [°], $\tau(\delta_\phi) \in \{0, 2, \dots, 10\}$ [s], $N(\Phi_{\mathfrak{S}_7}) = 5$, $N(S_6 \cdot \Gamma_5) = 264$.

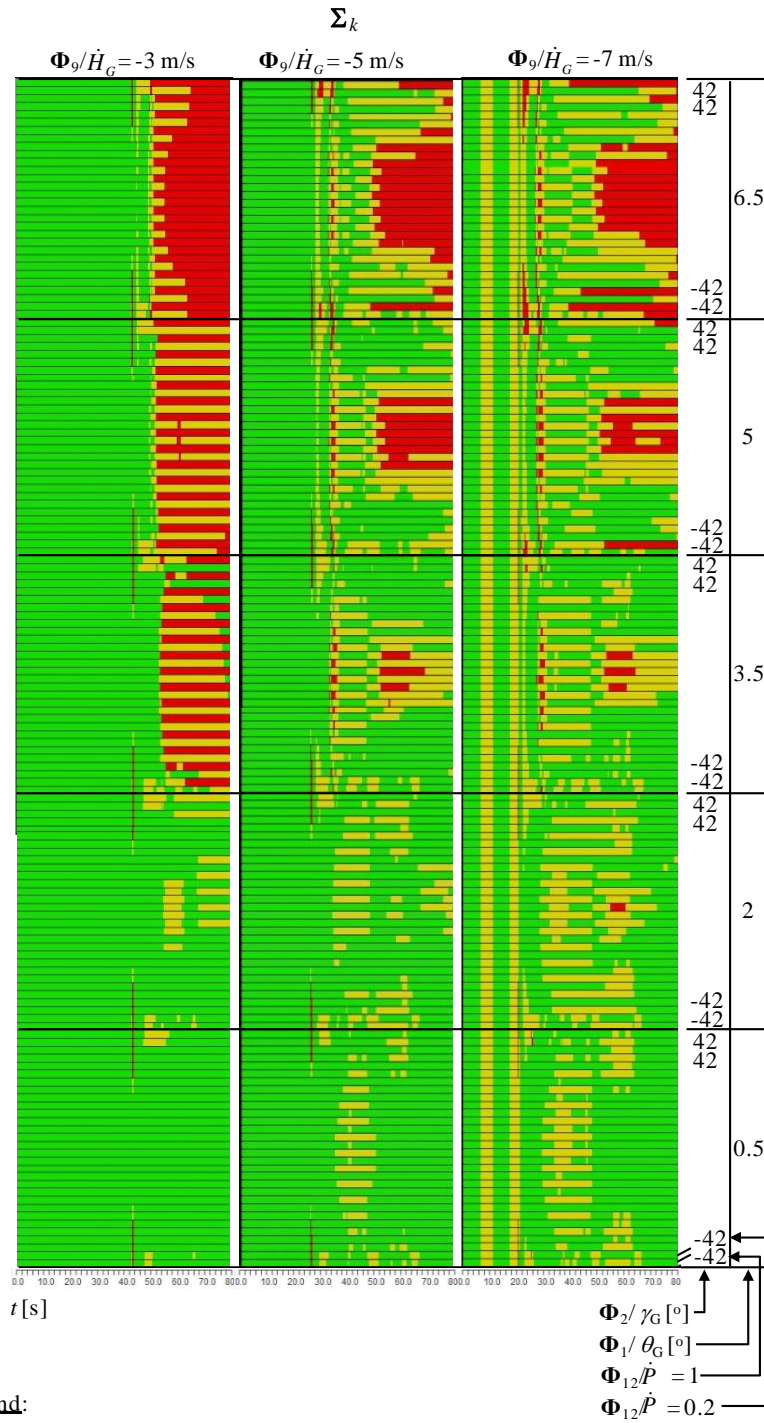
Figure 13 – Integral safety spectra for flight domain $\mathfrak{S}_7 \equiv S_6 \cdot \Gamma_5$: ‘Landing approach and go-around in wind shear conditions (Φ_6) with left-hand engine out (Φ_{11}). Errors in selecting (or variations of) go-around thrust increase delay (Φ_8), commanded flight path angle (Φ_1) and flaps-up delay (Φ_7)’.



Legend:

See Tables 9-13 and legend of Figure 9; $\mathfrak{S}_9 \equiv S_7 \cdot \Gamma_7 = \Phi_9 \times (\Phi_{13} + \Phi_{14}) \times \Phi_{15}$ or $\mathfrak{S}_9 = \dot{H}_G \times (H_{FL} + \Delta\delta_k) \times \dot{H}_{G1}$, $\dot{H}_G \in \{-6, -5.5, \dots, -3\}$ [m/s], $H_{FL} \in \{7, 8, \dots, 13\}$ [m], $\Delta\delta_k \in \{-12, -11, \dots, -6\}$ [°], $\dot{H}_{G1} \in \{-0.3, -0.2, -0.1\}$ [m/s], $N(\Phi_{\mathfrak{S}_9}) = 4$, $N(S_7 \cdot \Gamma_7) = 147$.

Figure 14 – Integral safety spectra for flight domain $\mathfrak{S}_9 \equiv S_7 \cdot \Gamma_7$: ‘Landing approach, landing and ground-roll. Errors in selecting (or variations of) commanded rate of descent (Φ_9), flare start altitude (Φ_{13}) together with elevator-up increment (Φ_{14}), and commanded glide slope (Φ_{15}) before touchdown’.

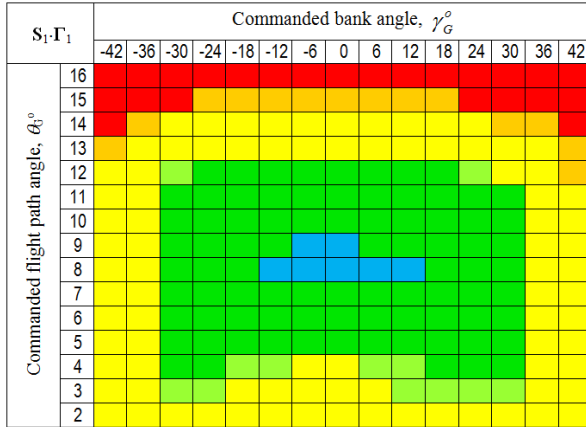


Legend:

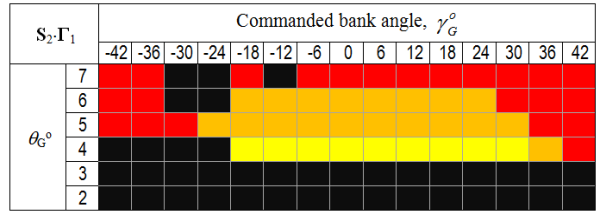
See Tables 9-13 and legend of Figure 9; $\mathfrak{S}_8 \equiv \mathfrak{S}_6 \cdot \Gamma_6 = \Phi_6 + \Phi_{11} + (\Phi_9 \times \Phi_1 \times \Phi_2 \times \Phi_{12})$ or $\mathfrak{S}_7 = k_W + \delta_{\gamma_2} + (\dot{H}_G \times \theta_G \times \gamma_G \times \dot{P})$, $k_W = 1$ – see Table 8, $\delta_{\gamma_2} = -5\% \dot{H}_G \in \{-3, -5, -7\}$ [m/s], $\theta_G \in \{0.5, 2, \dots, 6.5\}$ [°], $\gamma_G \in \{-42, -36, \dots, 42\}$ [°], $\dot{P} \in \{0.2, 1\}$ [-], $N(\Phi \mathfrak{S}_8) = 6$, $N(\mathfrak{S}_6 \cdot \Gamma_6) = 450$.

Figure 15 – Integral safety spectra for flight domain $\mathfrak{S}_8 \equiv \mathfrak{S}_6 \cdot \Gamma_6$: ‘Landing approach and go-around in wind shear conditions (Φ_6) with left-hand engine out (Φ_{11}). Errors in selecting (or variations of) commanded rate of descent (Φ_9), commanded flight path (Φ_1) and bank (Φ_2) angles, and right-hand engine thrust increase rate (Φ_{12}) in climb’.

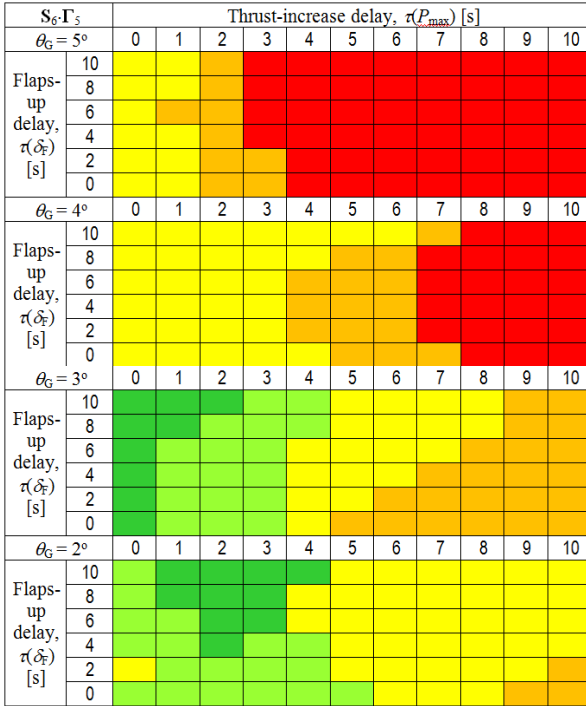
(a) Tree $\mathfrak{S}_1 \equiv \mathbf{S}_1 \cdot \Gamma_1$: Normal takeoff and initial climb. Errors in selecting (or variations of) commanded flight path and bank angles



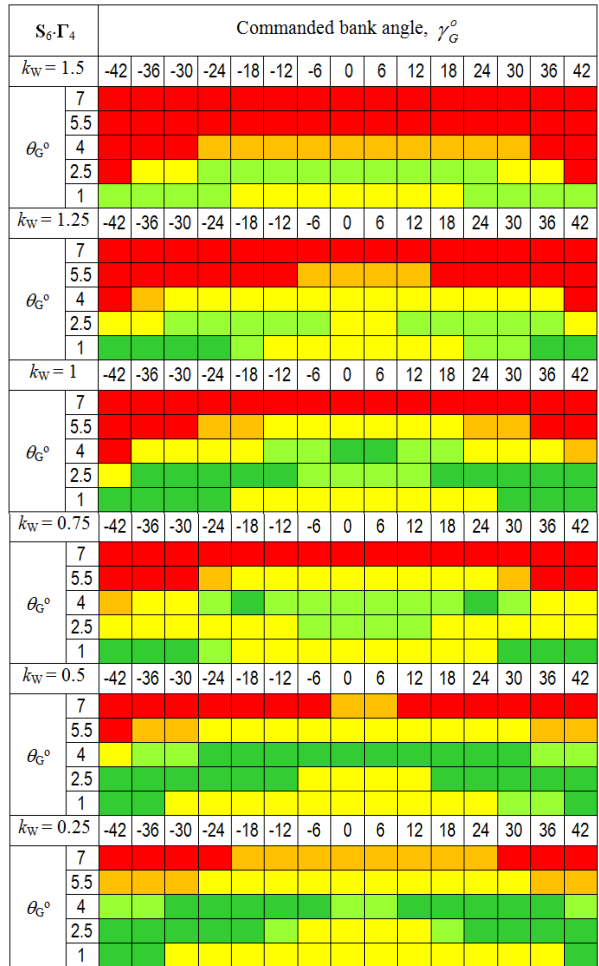
(b) Tree $\mathfrak{S}_2 \equiv \mathbf{S}_2 \cdot \Gamma_1$: Continued takeoff and initial climb, with left-hand engine out during ground-roll. Errors in selecting (or variations of) commanded flight path and bank angles



(c) Tree $\mathfrak{S}_7 \equiv \mathbf{S}_6 \cdot \Gamma_5$: Landing approach and go-around in wind shear conditions with left-hand engine out. Errors in selecting (or variations of) go-around thrust increase delay, flaps-up and commanded flight path angle



(d) Tree $\mathfrak{S}_6 \equiv \mathbf{S}_6 \cdot \Gamma_4$: Landing approach and go-around in wind shear conditions with left-hand engine out. Variations of wind shear intensity, and commanded flight path and bank angles



Legend: ■■■■ — color codes of main safety categories $\xi_k, \xi_k \in \{\text{I, II-a, II-b, III, IV, V}\}$ – see Table 1. ■ — ξ_T , see Fig. 2(a).

Figure 16 – Safety windows for mapping selected complex sub-domains of flight.